Photoconductivity of Thin Film Semiconductor as Compared to that of Bulk Semiconductor

By

Sagni Megersa Moti

April 2017

Photoconductivity of Thin Film Semiconductor as Compared to that of Bulk Semiconductor

By

Sagni Megersa Moti

Submitted in Partial fulfillment of the requirements for the degree of Master of Science in Physics
In the School of Applied Natural Science at Adama Science and Technology University

Advisor

Dr. Megersa Wodajo

April, 2017

Adama, Ethiopia

ADAMA SCIENCE AND TECHNOLOGY UNIVERSITY
POSTGRADUATE PROGRAM
SCHOOL OF APPLIED NATURAL SCIENCE
APPLIED PHYSICS PROGRAM

As thesis research advisor, I hereby certify that I have read and evaluated this thesis entitled: "**Photoconductivity of Thin Film Semiconductor as Compared to that of Bulk Semiconductor**" prepared under my guidance by Sagni Megersa. I recommend that it can be submitted as fulfilling the thesis requirement.

Dr. Megersa Wodajo	_____	_____
Advisor	Signature	Date

As members of the Board of Examiners of the M.Sc. thesis Open Defense Examination, we certify that we have read and evaluated the thesis work prepared by **Sagni Megersa** and examined the candidate. We recommended that the thesis be accepted as fulfilling the thesis requirement for the Degree of Master of Science in Physics.

_____	_____	_____
Chairperson	Signature	Date
_____	_____	_____
Internal Examiner	Signature	Date
_____	_____	_____
External Examiner	Signature	Date

Declaration and Statement of the Candidate

This thesis has been submitted in partial fulfillment of the requirements for M.Sc. degree at the ASTU. I solemnly declare that this thesis work is not submitted to any other institution anywhere for the award of any academic degree, diploma, or certificate.

Brief quotations from this thesis are allowable without special permission provided that accurate acknowledgement of source is made. Requests for permission for extended quotation from or reproduction of this manuscript in whole or in part may be granted by the head of major department or the Dean of the School of Graduate Studies when in his or her judgment the proposed use of the material is in the interests of scholarship. In all other instances, however, permission must be obtained from the author.

Name of candidate: Sagni Megersa Signature: _____

Place: Adama Science and Technology University, Adama

Date of Submission: April, 2017

Acknowledgements

First of all, I would like to give great thanks to almighty God who gave me this chance and helped me in all aspects for the successful accomplishment of my study.

Secondly, I would like to express my heartfelt gratitude to my advisor Dr. Megersa Wodajo who gave me the unique opportunity to make this thesis possible. I am very thankful to him for the interesting topic and his effective guidance and constructive comments throughout the study. I am also grateful for his insightful lectures that I took advantage of writing this thesis. I would like to thank the Nelson Mandela Metropolitan University, South Africa for their measuring of the majority carrier concentration for different doping levels GaSb samples.

Finally, I am grateful to my family and especially my sister Dibeshi Megersa, for her full support and encouragement during my study. For love and understanding I thank to my best friends for the strong advices, discussions, patience and their strong material and mental support throughout my in the campus.

Table of Contents

Contents **pages**

List of figures

Figures **pages**

Abbreviations and acronyms

b	Thickness
C_R	Radiative capture coefficient
e	Elementary charge
E	Energy bending
E_C	Conduction band energy
E_V	Valence band energy
E_{SF}	Fermi energy level at the surface
E_{BF}	Fermi energy level in the bulk
E_g	Band gap energy
E_i	Intrinsic Fermi energy
eV	Electron volt
Φ_0	Photon flux density
G_0	Photon absorption rate
h	Planck's constant
K_B	Boltzmann constant
m_n^*	Effective mass of electrons
m_p^*	Effective mass of holes
n	Electron density
n_i	Intrinsic carrier density
n_0	Electron density in thermal equilibrium
δn	Excess carrier concentration
N_a	Acceptor carrier density concentration
N_C	Effective density in the conduction band
N_V	Effective carrier density in the valence band
p	Hole density
p_0	Hole density in thermal equilibrium
R	Reflectivity
T	Temperature
x	Depth below surface
x_p	Penetration depth
α	Absorption coefficient
k_∞	Dielectric constant
ε_0	Permittivity of free space
π	Pi
τ_R	Radiative excess carrier lifetime

Abstract

In this study, the photo response of gallium antimonide (GaSb) thin film and bulk material is investigated under different conditions. First, with the aid of the principle of the illumination mechanism, the photon absorption rate as a function of absorption coefficient and depth below the illuminated surface in both the bulk and the thin films of GaSb were determined. Next, using the steady state condition of the free carriers generation-recombination mechanism, the radiative excess carrier lifetime of the photo-generated free carriers is described in both thin films and the bulk material as function of the depth below the surface, doping levels, injection levels and absorption coefficient. The obtained result indicates that, photon absorption rate and the free carrier's generation rate in general increases with decreasing the thickness of the thin films. The photo-response of the thin film semiconductor is found to be in general dominated by the property of the surface depletion layers of the material and hence extremely higher than the photo-response of the deep bulk.

Chapter 1

Introduction

Thin films are thin material layers ranging from fractions of a nanometer to several micrometers in thickness. The thickness is typically less than several microns [1]. Thin films of semiconductors have the main applications in electronic semiconductor devices and optical coatings. Some work is being done with ferromagnetic thin films as well for use as computer memory. Semiconductor materials exhibit a number of useful unique properties related to their electronic structure. They can be fabricated to be in bulk or in thin film forms. A semiconductor material is said to be in thin film form only when it is built up as a thin layer on a solid support called substrate by a controlled condensation of the individual atomic, molecular, or ionic species [2]. Thin films are also regarded as two dimensional materials fabricated by the process of condensation of atoms, molecules or ions. This is what makes them to have unique properties significantly different from their corresponding bulk materials. These unique properties are as a result of the changes that occur in their physical dimensions, geometry and microstructure [3].

In thin films there are deviations from the properties of the corresponding bulk materials that arise because of their small thickness, large surface-to-volume ratio and their unique physical structure which is a direct consequence of the growth process [4]. Most of the new thin film technologies coming up are based on the use of materials with very thin film geometry because they tend to lower costs and also lower material consumption [5]. Semiconducting thin film materials, which are based on sulfides and selenides have recently got much consideration as materials for optoelectronics technology. Thin films have other useful properties of electrical conduction, optical transmittance, reflectivity, and absorption and corrosion resistance.

During the recent decades, semiconductor materials are extremely vital in the development of wide range electronic and optoelectronic devices for information applications. A significant property of a semiconductor is its temperature dependence of conductivity, that is, the fact that the conductivity in semiconductors increases with increasing temperature, whereas the conductivity in metals decreases with increasing temperature [6].

Thin films are widely used in a large number of solid state devices. Some of these applications include photoconduction which is the change in the electrical conductivity of a substance, as a result of absorbing electromagnetic radiation [7]. The current investigation is the novel applications in which conversion of solar energy into electrical energy through photovoltaic effect cause photons that contain various amounts of energy corresponding to different wavelengths of light [8]. Many researchers [7, 9, 10] reported that as the thickness of the film increases, the absorption edge shifts towards lower energy region (higher wavelengths) and becomes much sharper (i.e. the band gap decreases). It has also been reported that films present a steep absorption edge at a wavelength of 500 nm with a band gap value of about 2.45 eV and their refractive index was of about 2 for the higher wavelengths while after annealing the absorption edge undergoes a slight shift towards the higher wavelengths [11].

Thin films can be used to fabricate optoelectronic devices that can convert photon energy into electrical energy for various uses. This can be achieved if their structure, inter-band transitions and other optical properties are maximized to harvest enough solar radiation to provide energy. Activities that take place when electrons transit between energy bands in thin films are a fundamental importance in harvesting solar radiation just like all fuels derive their source by utilizing solar energy [12]. Although solar energy is abundant it has not been harvested well. Obtaining energy by use of solar cells does not require sophisticated and expensive facilities. Thin film nanotechnology has been able to fabricate cheap opto-electronic devices that produce power for homes, small commercial uses or electric current for other uses [13]. It is a source of energy that is reliable, easy to maintain and even install and because of some of these advantages over other forms of fuels, there is a need to research on thin film materials with good photoelectrical properties in the visible range and those that extend into the IR and UV regions for photovoltaic cells [14]. Photovoltaic cells are known to absorb light (photons) from the sun and convert them directly into electricity. They consist of a p-type layer which has a majority hole carriers and an *n* type layer that has majority electron carrier. When a photon with energy greater than the band-gap of the semiconductor illuminates such a cell, it may be absorbed by the material and this takes the form of a band-to-band electronic transition producing an electron-hole pair [3].

When an electric field is applied to the material by an external voltage source, it causes the electrons and holes to be transported. Hence, Photoconductive materials can be used in the manufacturing of photoelectric devices. Typical photoconductive substances consist of germanium, gallium, selenium, or silicon with impurities, also known as dopants, added. Other common materials include metal oxides and sulfides. Currently, the global amount of information doubles every year. Many things we are taking for granted (such as, computers, Internet and mobile phones) would not be possible without silicon microelectronics. Since the beginning of semiconductor electronics, the number of transistors in an integrated circuit has been increasing exponentially with time [15].

One of the key parameters that often determine the range of applications of a given semiconductor is the basic energy band gap that separates the conduction from the valence bands, which is typically in the range from 0 to 3.5 eV for semiconductors [16]. In recent years, research on the preparation and characterization of thin films was developing into a major research area. Thus, the electronic industries due to the use of thin films in electronic, optoelectronic and other devices have become the supreme beneficiary of thin film technology.

The study of the optical generation and recombination of excess carriers in semiconductor is a crucial issue in study of the performance of the material. Recombination of charge carriers is the opposite of generation of charge carriers, representing mechanisms that reduce the excess charge density. When there is a generation of charge carriers, it is always balanced at steady-state condition by a recombination of charge carriers. The recombination of charge carriers takes place both in the bulk and at the surface of a semiconductor. The electron and the hole are no longer free carriers participating in electrical conduction. Thus, the concept of lifetime is introduced to estimate the time span of life of the carrier before its annihilation by recombination and also it provides information on how fast or slow the recombination of the minority carriers takes place in that semiconductor material. The lifetime referred to here is the minority carrier lifetime. Alternatively, the value of minority carrier lifetime provides a direct assessment of the quality of the material for various device applications [17, 18].

Photoconductivity is the tendency of a substance to conduct electricity to an extent that depends on the intensity of light-radiant energy (usually infrared transmission or visible light) striking the surface of a sample. Most semiconductor materials have this property [19]. The basic principle involved in photoconductivity is that, when photons of energy greater than that of the band gap of the semiconductors are incident on the material, electrons -hole pairs are created resulting in the enhancement of electrical conductivity [20]. The electrical conductivity of the material increases in proportion to the photon flux density of the illuminating light.

Photoconductivity is a useful tool to study the properties of semiconductors. It is also considered to be an important tool for providing information about the nature of the photo-excitations. A good photoconductive device requires efficient charge separation and efficient transport of charge carriers to electrode. The conductivity of the material depends upon the carrier density and complex process of carrier generation, trapping and recombination. It is also a function of temperature, intensity and energy of illuminating radiation [21].

The main objective of this thesis is to determine the factors affecting the photo-conductivity of thin film semiconductors and compares it with that of the bulk (thick) semiconductors. The specific objectives of this study includes, the photon absorption effect and the generation of excess carriers in both thin films and bulk semiconductors. Then, the generation of excess carriers (or photocurrent) in the thin film and thick semiconductors have been considered. Finally, the recombination mechanisms in both thin films and bulk semiconductors and the determination of excess carrier lifetimes in both thin films and bulk semiconductors are considered.

This thesis is organized as follows. The second chapter incorporates review of related literature. It is divided in to six sub sections. The third chapter deals with the methodologies followed to conduct the research. The fourth chapter presents analysis of data and discussion of the research work. Chapter five gives the conclusions of the research work.

Chapter 2

Literature Review

2.1 Energy bands in solids

Most semiconductors occur in solid form. These solids are made up of atoms which in turn contains electrons. From quantum mechanics it is clear that electrons of an isolated atom can have only discrete energy levels. When a number of atoms are brought together to form a crystal, their discrete energy levels split to form a band. As the inter-atomic spacing decreases these bands merge together to form a single band. When the distance between these atoms approaches equilibrium distance, the band splits again into two bands separated by a region called the forbidden gap (E_g). The forbidden gap separates the two energy state bands with the condition that no carriers can occupy energies within the forbidden gap. The upper band is called the conduction band (CB) with its minimum energy labelled as E_C and the lower band is called the valence band (VB) with its maximum energy labelled as E_V [22, 23].

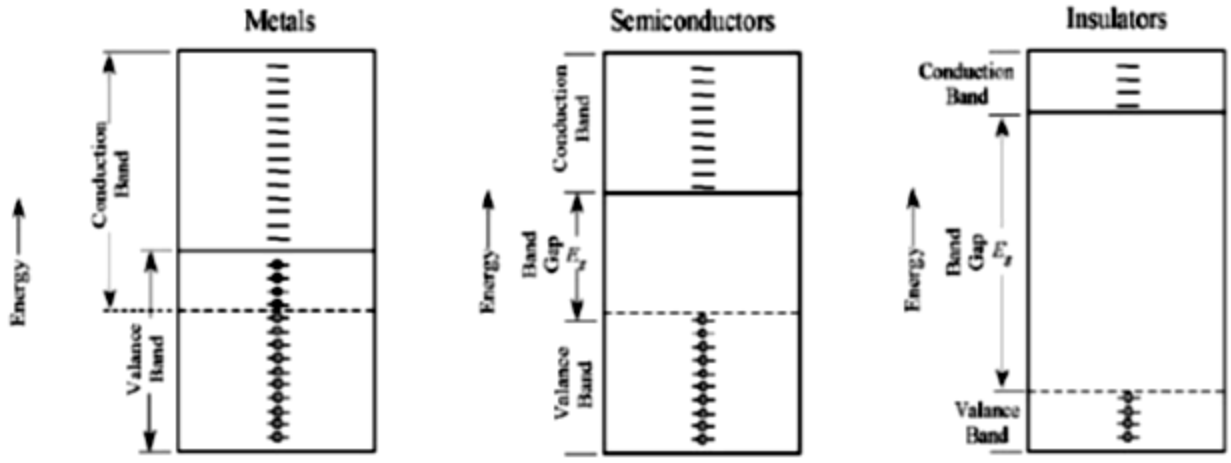

Figure 2.1: Band gaps for Metals, Semiconductors and Insulators [22].

In conductors (i.e. metals) as shown in Figure 2.1, the conduction band is either partially filled or overlaps the valence band so that there is no band-gap. This causes the uppermost electrons in the partially filled band or electrons at the top of the valence band to move to the next higher available energy level when they gain kinetic energy. Through this, current conduction readily occurs in conductors. In semiconductors, the bonds between

neighbouring atoms are only moderately strong. When thermal vibrations occur they break some of the bonds and free electrons along with free holes are produced. That is, why the band gap of a semiconductor is not as large as that of an insulator. Therefore, some electrons will be able to move from the valence band to the conduction band leaving holes in the valence band. If an electric field is applied, then both the electrons in the conduction band and the holes in the valence band will gain kinetic energy and conduct electricity. The valence electrons form strong bonds between neighboring atoms in insulators. These strong bonds are difficult to break. This means that there are no free electrons to participate in current conduction. This causes the band gap in an insulator to be large. When we consider the band gap in an insulator, thermal energy or any external applied electric field cannot raise the uppermost electron in the valence band to the conduction band [13].

The band gap energy, $E_g = E_C - E_V$, is perhaps the most important in semiconductor physics. A contraction of the crystal lattice with decreasing temperature usually leads to a strengthening of the interatomic bonds and an associated increase in the band gap energy. The first empirical relation for the band gap shift with temperature was developed by Varshni *et al* [24, 25, 26]:

$$E_g(T) = E_g(0) - \frac{\alpha T^2}{T + \beta}. \tag{2.1}$$

where $E_g(0)$ is 0.813 eV at 0 K, $\alpha = 3.78 \times 10^{-4}$ eV/K, $\beta = 94$ K and the band gap energy at the normal temperature (300 K) is equal to 0.726 eV for a GaSb semiconductor.

Figure 2.2, illustrates the temperature dependence of band gap energy along with E_C and E_V. As one can see from Figure 2.2, both E_C and E_V become closer and closer to the mid-gap with increasing temperature, as a result the band gap energy decreases with increasing temperature.

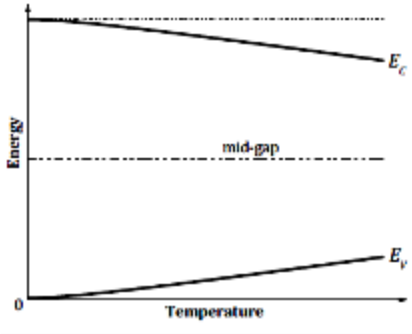

Figure 2.2: Temperature dependence of band gap energy along with E_C and E_V.

Materials are classified as direct or indirect semiconductors depending on their band structure. Figure 2.3 illustrates indirect and direct band gap structure of semiconductors. As one can see from Figure 2.3 (a), the maximum in the valence band (E_V) occurs at the center of the

Brillouin zone or zero momentum ($k = 0$), while the minimum in the conduction band occurs along the [100] direction at P_C different from zero (or $k \neq 0$), where k is the wave number. The electron at the conduction band minimum (E_C) with zero kinetic energy can have crystal momentum different from zero (i.e. P_C). When an electron makes a transition from the valence band to the conduction band it requires then, not only an energy change is greater than E_g, but also some change in the crystal momentum, $p = \hbar k$. This makes such semiconductors to be indirect semiconductors because a change in crystal momentum is required in their transitions. One can see from Figure 2.3 (b) that the maximum in the valence band and the minimum in the conduction band occurs at the center of the Brillouin zone (or $k = 0$) and in this case, an electron making a transition from the valence band to the conduction band can do so without a change in its momentum. Such semiconductors are classified as direct band gap semiconductors because the transition from the valence band to the conduction band does not require a change in crystal momentum for the electrons.

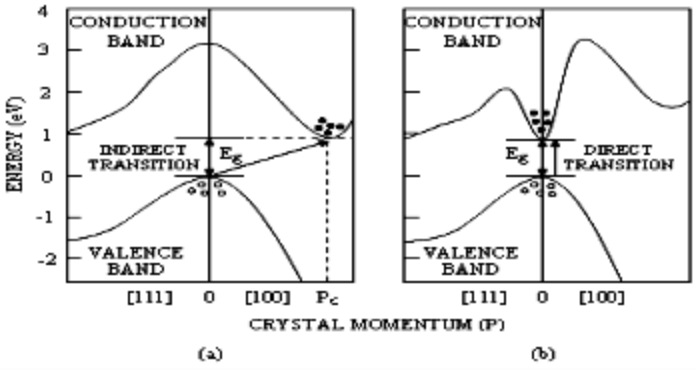

Figure 2.3: (a) Indirect and (b) direct bandgap structures of semiconductors [27].

2.2 Densities of Charge carriers

The density of states function can be applied to electrons in the conduction band and holes in the valence band of a semiconductor. This can be done by assuming parabolic bands for both the conduction and valence bands and using the conduction and valence band edge as a reference level. Since the densities of states are the properties of the conduction and the valence bands, they are not affected by the variation of Fermi level position in the band gap. Figure 2.4 illustrates the room temperature energy dependence of the densities of states in the

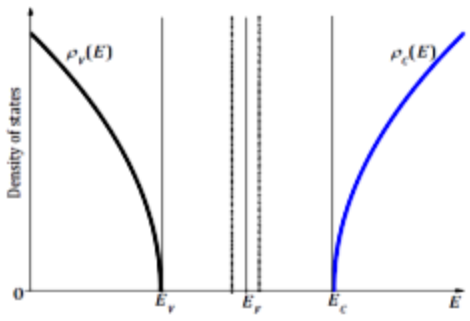

Figure 2.4: Energy dependence of the densities of states in the conduction and the valence-bands.

conduction and the valence bands. As can be seen from Figure 2.4 the densities of states attains their minimum values (zero values) at the band edges. The density of states in the valence band increases going deep into the band with decreasing energy, and the density of states in the conduction band increases going deep in the band with increasing energy.

The general expressions for the equilibrium densities of electrons and holes in a semiconductor can be derived using the density of states function and the Fermi–Dirac (F-D) distribution function. If one assumes that the constant energy surfaces near the bottom of the conduction band and the top of the valence band are spherical, then the equilibrium distribution functions for electrons in the conduction band and holes in the valence band may be described in terms of the F-D distribution function. The number of electrons excited across the gap can then be calculated from the Fermi-Dirac probability distribution as [28]:

$$f_n(E) = \frac{1}{1 + \exp\left(\frac{E - E_F}{k_B T}\right)}, \tag{2.2}$$

where E is the energy of the charge carrier and E_F is the Fermi energy level.
The F-D distribution function for holes in the valence band is also expressed by:

$$f_p(E) = 1 - f_n(E) \approx \frac{1}{1 + \exp\left(\frac{E_F - E}{k_B T}\right)}, \tag{2.3}$$

The equilibrium concentration of electrons in the conduction band and holes in the valence band of a material can then be calculated using Eqns.(2.4) and (2.5) shown below. The intrinsic density of electrons (n_i) is calculated using the density of states in the conduction band, N_C, as well as the Fermi and conduction band energies. The intrinsic density of holes is calculated based on the properties of the valence band. Using the bottom of conduction band as E_C and the top of valance band as E_V, the electron density in the conduction band can then be given by [22, 23]:

$$n_0 = N_C \exp\left(-\frac{E_C - E_F}{\mathrm{k_B T}}\right), \tag{2.4}$$

In a similarly way, the hole density in the valence band can be given by:

$$p_0 = N_V \exp\left(-\frac{E_F - E_V}{\mathrm{k_B T}}\right), \tag{2.5}$$

where N_C and N_V are the effective density of states in the conduction and valence bands respectively and their expression as a function of temperature is given as:

$$N_C = 2\left(\frac{2\pi m_n^* k_B T}{h^2}\right)^{3/2}, \tag{2.6}$$

and

$$N_V = 2\left(\frac{2\pi m_p^* k_B T}{h^2}\right)^{3/2}, \tag{2.7}$$

where m_n^* and m_p^* are electron and hole effective masses in the conduction and valence bands respectively. Since there are equal amounts of intrinsic holes and electrons, Eqns. (2.4) and (2.5) can be combined to show that the intrinsic carrier concentration is not dependent on the intrinsic Fermi energy, but it is dependent on the size of the energy gap (E_g) and the result is given by:

$$n_i = \sqrt{N_C N_V} Exp\left(-\frac{E_g}{2k_B T}\right). \tag{2.8}$$

2.3 Intrinsic semiconductors

Intrinsic semiconductors are pure crystals of semiconductor materials. Conduction in these materials is due to the intrinsic processes without the influence of impurities. It occurs due to the electrons that are excited from the top of the valence band to the bottom of the conduction band by thermal energy. Thus, a semiconductor may be considered as an intrinsic semiconductor, if its thermally generated carrier density represented by n_i is much larger than the background doping or residual impurity densities. At $\Delta T = 0$ K, an intrinsic semiconductor behaves like an insulator because the conduction band states are totally empty and the valence band states are completely filled. However, as the temperature increases, some of the electrons in the valence band states are excited into the conduction band states by thermal energy, leaving behind an equal number of holes in the valence band. Suppose that $\mathcal{R}$ is the concentration of electron-hole pairs thermally generated in the

respective bands and $\mathcal{R}_R$ is the concentration of electron-hole pairs annihilated after the generation, the free carrier concentrations in the conduction and valence bands adjust for the intrinsic semiconductor to:

$$n_0 \approx \mathcal{R} - \mathcal{R}_R = p_0 = n_i. \tag{2.9}$$

where n_0 and p_0 denote the equilibrium electron and hole densities, respectively. Since the nondegenerate relations are obviously valid for an intrinsic semiconductor where the Fermi level (E_F) is equal to the intrinsic level energy (E_i) in the semiconductor.

When an external field is applied, the electrons that are excited into the conduction band by thermal means accelerate using the vacant states available in the conduction band. At the same time the holes in the valence band move but in a direction opposite that of the electrons. Since the non-degenerate relations are obviously valid for an intrinsic semiconductor where the Fermi level, E_F is equal to the intrinsic level energy, E_i in the semiconductor, one can write Eqns.(2.4) and (2.5) that:

$$n_i = N_C exp\left(-\frac{E_C - E_i}{k_B T}\right) = N_V exp\left(-\frac{E_i - E_V}{k_B T}\right). \tag{2.10}$$

Taking into account Eqns.(2.6) and (2.7) along with Eqn.(2.10) gives:

$$E_i = \frac{E_C + E_V}{2} + \frac{3}{4}(k_B T) ln\left(\frac{m_p^*}{m_n^*}\right). \tag{2.11}$$

where m_p^* , m_n^* and E_g are known at a given temperature.

Figure 2.5 illustrates the carrier density and energy band structure for intrinsic *p*-type semiconductor ($m_p^* > m_n^*$) at (a) zero *T*, (b) intermediate *T* and (d) high *T*. The intrinsic carrier density increases with increasing temperature.

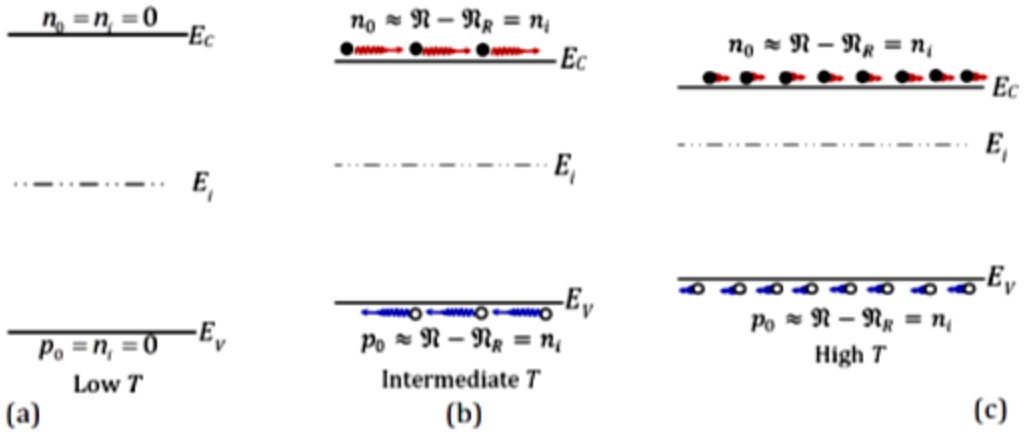

Figure 2.5: Carriers density and energy band structure for intrinsic semiconductor at (a) low T, (b) intermediate T and (c) high T.

Figure 2.6 also shows the temperature dependence of the intrinsic Fermi-level, E_i, Conduction band edge, E_C and valence band edge, E_V. One can easily see from Figure 2.6 that, if the electron and hole effective masses are equal, $m_p^* = m_n^*$, the intrinsic Fermi level, E_i is exactly in the Centre of the band gap. The intrinsic Fermi level, E_i moves toward the conduction band edge if $m_p^* > m_n^*$ and toward the valence band edge if $m_p^* < m_n^*$. One can also see that, the energy band gap also decreases with increasing temperature.

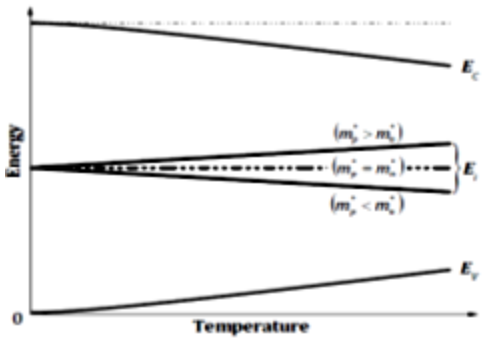

Figure 2.6: Temperature dependence of intrinsic Fermi level, E_i, in the band gap energy of a semiconductor for $m_p^* = m_n^*$, $m_p^* > m_n^*$ and $m_p^* < m_n^*$

2.4 Extrinsic semiconductors

If a dopant (impurity) is introduced into an intrinsic semiconductor, then it changes and becomes an extrinsic semiconductor. The process of deliberate addition of controlled quantities of impurities to a pure semiconductor is called doping.

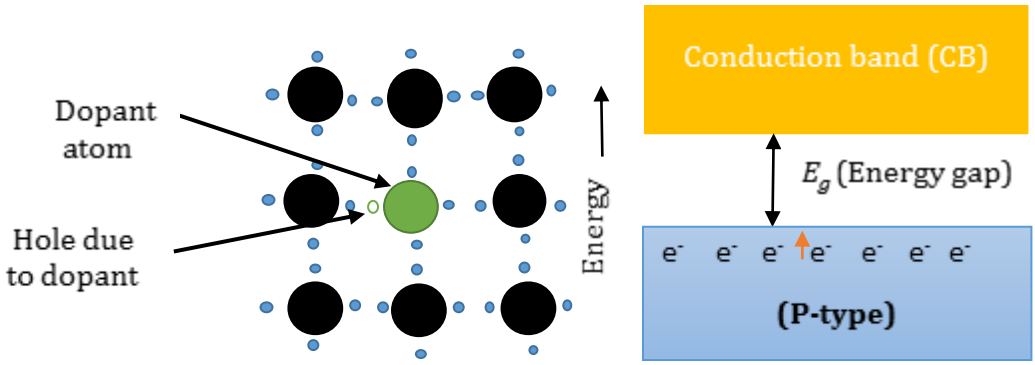

Figure 2.7: p–type doped semiconductor with an acceptor [29].

If the doping process results into a p-type semiconductor then the impurity atoms are called acceptors and the energy levels of these holes are called the acceptor energy levels (E_a).

The addition of impurities (doping) greatly increases the conductivity of most semiconductors as illustrated in Figure 2.8 [28]. The most important and unique feature of a semiconductor material lies in the fact that its electrical conductivity can be readily changed by many orders of magnitude by simply doping the semiconductor with shallow-donor or shallow-acceptor impurities. By incorporating the doping impurities into a semiconductor, the electron or hole density will increase with increasing shallow-donor or shallow-acceptor impurity concentrations. If a group-III element is introduced into a group-IV elemental semiconductor, then there is a deficiency of one electron for each replaced host atom by a group-III impurity atom, leaving an empty state (or creation of a hole) in the valence band. Hence, the conduction process is carried out by holes in the valence bands, and the semiconductor is called a p-type semiconductor. The group-III elements including boron, gallium, and aluminum are common doping impurities for producing p-type doping in the elemental semiconductors. Thus, group-III elements are shallow-acceptor impurities for the elemental semiconductors.

To excite electrons from the donor level into conduction band (CB) or holes from acceptor level into valence band (VB), energy known as ionization energy is required. The ionization energy (E_i) of donor electrons is approximately the same as the ionization energy of acceptor holes in the same crystal. When it is compared to the energy gap, the ionizatio n energy of an impurity atom is very small. This means that at room temperature a large

fraction of the donor level electrons as well as acceptor level holes are excited into the conduction and valence band respectively. This fraction is much larger than the fraction of electrons excited from the valence band or that of holes created by these electr ons due to the thermal energy [28]. The product of the number of electrons in the conduction band and the number of holes in the valence band must be constant for any semiconductor according to the law of mass action [30]. The number of electrons in the *p*-type semiconductor is reduced causing the holes in the valence band to become the majority charge carriers.

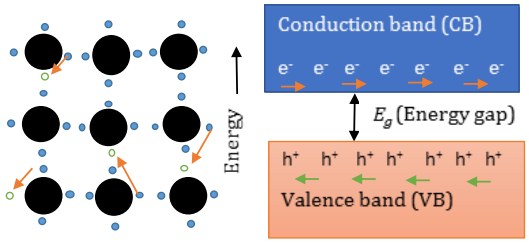

Figure 2.8: Movement of electrons and holes during conduction [29].

The Fermi level (E_F) with higher donor concentration (N_D) will move closer to the bottom of the conduction band and in the same manner the one with a higher acceptor concentration will move closer to the top of valence band [2]. Hence, the electron and hole densities in extrinsic semiconductors can be expressed as:

$$n_0 = n_i exp\left(\frac{E_F - E_i}{K_B T}\right), \tag{2.12}$$

and

$$p_0 = n_i exp\left(\frac{E_i - E_F}{K_B T}\right), \tag{2.13}$$

If both the donor and acceptor impurities are present simultaneously, then the fermi level must adjust itself in such a way so as to preserve charge neutrality.

If a material is doped so heavily that the Fermi energy is in one of the bands, the material is referred to as degenerately doped. This happens in n-type materials when the donor density is greater than the density of states in the conduction band and in p-type materials when the acceptor density is greater than the density of states in the valence band [31].

2.5 The near surface region at thermal equilibrium

The bulk of most isolated III-V semiconductors have three various regions of different carrier concentrations. This consists of a neutral region (with high thermal equilibrium

majority carrier concentration), followed by a transition layer (with decreasing thermal equilibrium majority carrier concentration in moving towards the surface), and a depleted surface region of very low thermal equilibrium majority carrier concentration. The width of the total depletion layer (b_1) between the surface and the neutral region is given by the sum of the width of the highly depleted layer (b_s) and the width of the transition region (b_δ) between the highly depleted region and the quasi-neutral region:

$$b_1 = b_s + b_\delta \,. \tag{2.14}$$

The band bending in different layers accounts for the variation of the majority carrier concentrations in these layers. The description of the band bending, E(x) at any location x in the depletion region also enables us to evaluate the thermal equilibrium free carriers densities at any point x in the depletion region. The majority carrier density, $p\ (E)$ at any energy, E in the depletion layer of a p-type semiconductor can be expressed as [32]:

$$p\ (E) = p_0\ \exp\left(-\frac{E}{k_B T}\right). \tag{2.15}$$

The majority carrier concentration in Eqn.(2.15) is in general decreases with increasing the band bending. The minority carrier concentration at any point in the depletion layer can be described using the law of mass action and along with Eqn.(2.15) as:

$$n\ (E) = n_0\ \exp\left(\frac{E}{k_B T}\right). \tag{2.16}$$

Hence, the position dependence of the bending in energy in the entire depletion layer between the surface and the edge of the quasi-neutral region can be approximated in general as [32, 33]:

$$E(x) = \ -\frac{e^2 N_a}{2k_\infty \varepsilon_0}(b_1 - x)^2. \tag{2.17}$$

where $E(x)$ is the band bending at depth x, N_a is doping concentration, k_∞ is dielectric constant (1.44×10^1) and ε_0 is permittivity of free space $\left(8.85 \times 10^{-12}\ {}^{c^2}/_{Jm}\right)$. Figure 2.9 describes the position dependence of the energy bending in the entire depletion layer between the surface and quasi-neutral region in a thin film semiconductor. The position dependence of the energy bending in the depletion layer can be determined using Eqn.(2.17).

From this figure it can be seen that the energy bending in the thick (bulk) region remains fixed with doping level. However, in the entire depletion layer the energy bends down and reaches its maximum at the surface. This is due to the fact that the majority carrier concentration in the depletion layer decreases from maximum value p_0 at the edge of the quasi-neutral region towards the surface and attains its minimum value in the entire region between the edge of the transition region and the surface. From Figure 2.9 we also observe that as the doping concentration increases while the energy bending decreases at the two surfaces of a thin film semiconductor. Moreover, it is seen from the figure that the widths of the depletion region in general decrease with increasing the doping level.

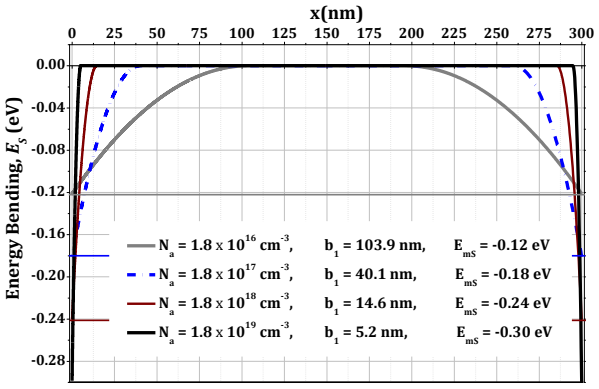

Figure 2.9: Energy bending against depth below the surface with different doping concentration in the thin film semiconductor.

The valence band maximum (VBM) in the neutral region (bulk) is represented by E_{BV} and that at the surface is represented by E_{SV}. The respective conduction band minimum (CBM) in the neutral region (bulk) and at the surface are represented by E_{BC} and E_{SC}. The totalband bending at the surface is represented by $E(0) = E_S$. The Fermi-level position relative to the valence band maximum (VBM) is denoted by E_{BF} in the bulk and by E_{SF} at the surface. The Fermi and the intrinsic energy levels in the entire sample are also represented by E_F and E_i, respectively. The thermal equilibrium majority carrier density p_{0s} under the surface of a p-type semiconductor can also be expressed in terms of the surface Fermi-level position, E_{SF} using Eqn.(2.19) as:

$$p_{0s} = p(E_s) = p_0 \exp\left(-\frac{E_s}{k_B T}\right). \tag{2.18}$$

Equation that relates the band bending and the Fermi-level position at the surface of a p-type semiconductor is given by:

$$E_{SF} = E_{BF} + E_S \,. \tag{2.19}$$

where the Fermi-level position, E_{BF} relative to the VBM in the bulk at room temperature for highly doped p-type semiconductor is given by:

$$E_{BF} = E_i - k_B T \ln\left(\frac{p_0}{n_i}\right). \quad (2.20)$$

2.6 Photo-response of semiconductors

The energy is needed to free an electron from the nucleus and thus create one electron hole pair. This energy can be supplied in the form of light. Each light photon has energy

$$E_{ph} = h\nu. \quad (2.21)$$

where h is the Planck's constant and ν is the frequency of the light. A semiconductor can absorb a photons having $h\nu > E_g$. The energy of each absorbed photon is consumed by raising a valence band electron in to the conduction band and creating one electron and one hole. Photon with $h\nu < E_g$ are basically not absorbed by the semiconductor and cannot generate electron-hole pair [34].

Photons incident on the surface of a semiconductor are either reflected from the top surface or absorbed in the material. The absorbed photon has the possibility of exciting an electron from the valence band to the conduction band. A key factor in determining if a photon is absorbed or transmitted is the amount of energy of the photon. Therefore, only if the photon has enough energy will the electron be excited into the conduction band from the valence band. Thus, absorption of photons creates both a majority and a minority carrier.

When the surface of a semiconductor is illuminated by a light source with $h\nu > E_g$ and the incident photon flux density, Φ_0 (number of incident photon per unit area per unit time), the fraction of the photons flux density reflected back is given by $\Phi_0 R$ and the fraction entering the sample is $\Phi_0(1-R)$, where R is the reflection coefficient (reflectivity) and can be defined in terms of the index of refraction of the media on either side of the surfaces (interfaces). Hence, it is calculated by using the relation [35, 36, 25]:

$$R = \left(\frac{n-1}{n+1}\right)^2. \quad (2.22)$$

Equation (2.22) assumes the refractive index, n remains constant for the entire wavelength range under consideration, i.e. $\lambda < 20\mu m$. For GaSb, the refractive index was taken as 3.8. This results in a typical value of R to be approximately 0.34.

A photon can excite an electron from an occupied state in the valence band to an unoccupied state in the conduction band. This is called an inter-band transition. In this case, an excited electronic state is formed in the conduction band and a hole is left behind. This is regarded as intrinsic excitation of free carriers. On the other hand, electrons can be excited from impurity centers within the forbidden energy gap to the conduction band by the photons with $h\upsilon < E_g$. This is also known as extrinsic excitation of free carriers. In this case, an excited electronic state is formed in the conduction band and an ionized state is left behind at the impurity center. Thus, photoconductivity in semiconductors may also be due to both either intrinsic or extrinsic excitations [37].

2.6.1 Absorption in infinitely thick semiconductor

Next, we are going to investigate a photon absorption rate at the surface and in the bulk of a very thick semiconductor. Thick (bulk) semiconductor refers to the case when the thickness of the semiconductor, b is infinitely large ($b \to \infty$). Figure 2.10 shows a photon beam of flux density Φ_0 directed at the upper surface of a portion of a semiconductor sample of width w and infinitely large thickness. It is assumed that the beam contains only photons of energy $h\upsilon \geq E_g$, selected by a monochromator. For clarity, the rays are shown for oblique incidence. However, based on the experimental set-up used to characterize the samples, a normal incidence is assumed for all reflection and transmission calculations in this work.

As the beam passes through the sample, the photon flux density at a distance x from the surface can be calculated by considering the probability of absorption within any infinitesimal thickness dx. The photon absorption rate at depth x for a given wavelength is proportional to the photon flux density, $\Phi(x)$ remaining at x after being absorbed in the preceding section of the material:

$$g_0(x) = \frac{d\Phi(x)}{dx} = -\alpha\Phi(x), \tag{2.23}$$

where α is a constant called the absorption coefficient, which is related to the dielectric properties of the material and the wavelength of the incident photon. The value of the absorption coefficient is determined using its dependence on the photon energy, analyzed by Bardeen *et al.* [38, 39]:

$$\alpha(\omega) = \frac{2^{\frac{2}{3}} m_n e^2}{3\hbar^2\sqrt{k_\infty}} \left(\frac{m_n^* m_p^*}{m_n(m_n^* + m_p^*)}\right)^{\frac{3}{2}} \left(1 + \frac{m_n}{m_n^*} + \frac{m_n}{m_p^*}\right) \left(\frac{h\upsilon - E_g}{m_n c^2}\right)^{\frac{1}{2}}. \quad (2.24)$$

Here, $\hbar = \frac{h}{2\pi}$ is the reduced Plank's constant, e is the elementary charge, m_n is the free electron mass, c is the speed of light and $m^*_{n/p}$ is the effective electron/hole mass.

The photon flux density $\Phi(\alpha, x)$, detected at depth x below the eliminated surface can be found by integrating Eqn. (2.23) from the surface to depth x as [40, 41]:

$$\Phi(\alpha, x) = \Phi_0(1 - R)e^{-\alpha x}, \quad (2.25)$$

Eqn. (2.25) is called Beer's Lambert law.

Many authors simply use the Lambert-Beer law, Eqn.(2.25) which predict an exponential decrease of the photon flux density with increasing the depth x and α. Figure 2.10 depicts how photons are absorbed in infinitely thick semiconductor. Note that, $\Phi(\alpha, x)$ has minimum value (0) for $\alpha x \to \infty$ and maximum value $(\Phi_0(1 - R))$ for $\alpha x \to 0$. This shows that, photons with high absorption coefficients are fully absorbed near the surface and photons with small absorption coefficients can go deep into the semiconductor.

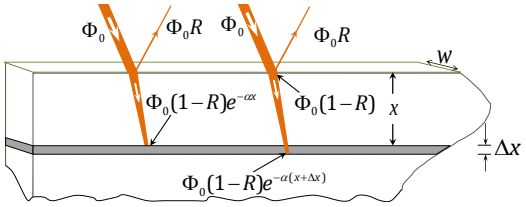

Figure 2.10: Absorption of photons in an infinitely thick semiconductor.

The total absorbed photon flux density in the layer of thickness, Δx is given by the difference between the photon flux density detected at depths x and $x + \Delta x$ below the illuminated surface as:

$$\Delta\Phi(\alpha, x, \Delta x) = \Phi_0(1 - R)e^{-\alpha x}(1 - e^{-\alpha \Delta x}), \quad (2.26)$$

If the elemental layer of thickness Δx is closer to the surface, then $x \to 0$, Eqn.(2.26) becomes:

$$\Delta\Phi(\alpha, \Delta x) = \Phi_0(1 - R)(1 - e^{-\alpha \Delta x}), \quad (2.27)$$

The total absorbed photon flux density in the entire sample can be obtained by letting $\Delta x \approx b \to \infty$ in Eqn.(2.27) as:

$$\Delta\Phi = \Phi_0(1-R). \tag{2.28}$$

If the depth x increases, $\Delta\Phi$ decreases and becomes zero for $x \to \infty$. For very small $\alpha\Delta x$, the term in the bracket on the right side of Eqn.(2.26) becomes $1 - e^{-\alpha\Delta x} \approx \alpha\Delta x$ and hence:

$$\Delta\Phi(\alpha, x, \Delta x) = \Phi_0(1-R)e^{-\alpha x}\alpha\Delta x. \tag{2.29}$$

Equation (2.29) represents the photon flux density absorbed in elemental layer of thickness Δx situated at depth x below the illuminated surface for a photon of very small absorption coefficient or energy ($\alpha \to 0$) or if the thickness of the layer, Δx is closer to zero ($\Delta x \to 0$). The photon absorption rate in the elemental layer of thickness, Δx of the semiconductor can be determined as:

$$g_0 = \frac{\Delta N_{ph}}{A\Delta x\Delta t} = \frac{\Delta\Phi}{\Delta x}, \tag{2.30}$$

Where ΔN_{ph} is the number of absorbed photons, A is the illuminated area of the sample, Δt is the time of illumination and $\Delta\Phi$ is the absorbed photon flux density given by:

$$\Delta\Phi = \frac{\Delta N_{ph}}{A\Delta t}, \tag{2.31}$$

For $\Delta x \to 0$, Eqn. (2.30) above takes the form:

$$g_0 = \frac{d\Phi}{dx}. \tag{2.32}$$

Taking into account Eqn. (2.32) along with Eqn. (2.25) yields the photon absorption rate at a point at depth x below the illuminated surface in very thick semiconductor to be:

$$g_0(\alpha, x) = \Phi_0(1-R)\alpha e^{-\alpha x} = \alpha\Phi(\alpha, x). \tag{2.33}$$

A close examination of Eqn. (2.33) reveals that, $g_0(\alpha, x) \to 0$ for both lower values of the absorption coefficient ($\alpha \to 0$) and higher values the absorption coefficient ($\alpha \to \infty$). That means, $g_0(\alpha, x)$ has maximum value at some finite value of $\alpha > 0$. The depth at which maximum absorption rate of photons can take place in the semiconductor for a given absorption coefficient, α can be determined by differentiate Eqn.(2.33) with respect to α and letting the result to be zero:

$$\frac{dg_0}{d\alpha} = (1-\alpha x)\Phi(\alpha,x) = 0. \tag{2.34}$$

(Since $\Phi(\alpha,x)$ can be zero only for large values of absorption coefficient ($\alpha \to \infty$) as discussed earlier, and) therefore $1-\alpha x = 0$ or $1 = \alpha x$ for all values of α. This defines a depth x below the illuminated surface where the maximum absorption rate occurs for a specific wavelength of light. The depth x at which $g_0\ (\alpha,x)$ has a maximum value for a given photon energy is called the penetration depth, x_p of that photon in the semiconductor. The penetration depth, x_p for a photon of particular absorption coefficient, α is hence given by:

$$x_p = \frac{1}{\alpha}. \tag{2.35}$$

Taking into account Eqn. (2.33) along with Eqn. (2.35) yields:

$$g_0(x,x_p) = \frac{\Phi_0(1-R)}{x_p}\exp\left(-\frac{x}{x_p}\right). \tag{2.36}$$

The maximum value of the absorption rate at the penetration depth, x_p for a photon with particular absorption coefficient, α can be determined using Eqns.(2.36) and (2.35) as:

$$g_0(x_p) = \frac{\Phi_0(1-R)}{x_p}\exp(-1) = 0.37\left(\frac{\Phi_0(1-R)}{x_p}\right). \tag{2.37}$$

The photon absorption rate in Eqn. (2.37) has maximum value at the surface (when $x \to 0$):

$$g_0(x_p) = \frac{\Phi_0(1-R)}{x_p}. \tag{2.38}$$

Hence, comparison of Eqns. (2.38) and (2.37) enables us to reach the conclusion that, the value of the photon absorption rate at the penetration depth is 37% the maximum value at the surface for all the photons. The limiting cases for the photon absorption rate in a very thick semiconductor can be concluded as:

$$g_0(x_p) = \begin{cases} \alpha\Phi_0(1-R), & \text{for } x \ll x_p, \\ 0.37\alpha\Phi_0(1-R), & \text{for } x = x_p, \\ 0, & \text{for } x \gg x_p. \end{cases} \tag{2.39}$$

2.6.2 Absorption in thin films semiconductors

The distinctive features of semiconductor thin films and bulk materials arise mainly due to the different between their dimensions. Since semiconductor thin films are ranging from fractions of a nanometer to several micrometers in their thicknesses, multiple reflections and transmissions of photons can occur at both the top and the bottom surfaces when they are illuminated. Very thin semiconductor films are mainly dominated by the under surface depletion layers, so that their photo-response is surface influenced than the bulk. Figure 2.11 shows a photon beam of energy, $hv \geq E_g$ and flux density, Φ_0 directed at the upper surface of a portion of a semiconductor sample of thickness b. Each time the radiation meets a surface, some photons are reflected and some are transmitted. The processes of reflection, transmission and absorption are repeated many times until all the photons are absorbed by the material and transmitted through the surfaces.

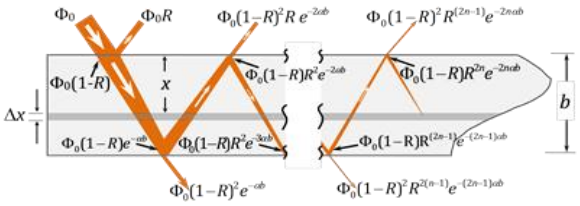

Figure 2.11: Absorption of photons in thin film semiconductor

The photon flux density transmitted through the bottom surface after n^{th} order is given by:

$$\Phi_{BT,n} = \Phi_0(1-R)^2 R^{2(n-1)} e^{-(2n-1)\alpha b}, \qquad (n = 1, 2, 3 \ldots). \tag{2.40}$$

The photon flux density reflected back to the sample from the bottom surface after n^{th} order is given by:

$$\Phi_{BR,n} = \Phi_0(1-R) R^{(2n-1)} e^{-(2n-1)\alpha b}, \qquad (n = 1, 2, 3 \ldots). \tag{2.41}$$

The photon flux density transmitted through the upper surface after n^{th} order is given by:

$$\Phi_{UT,n} = \Phi_0(1-R)^2 R^{(2n-1)} e^{-2n\alpha b}, \qquad (n = 1, 2, 3 \ldots). \tag{2.42}$$

The photon flux density reflected back to the sample from the upper surface after n^{th} order is given by:

$$\Phi_{UR,n} = \Phi_0(1-R)^2 R^{2n} e^{-2n\alpha b}, \qquad (n = 1, 2, 3 \dots). \tag{2.43}$$

The total photon flux density absorbed in the entire sample is hence given by:

$$\Delta\Phi = \Phi_0 - \Phi_0 R - \sum_{n=1}^{\infty} \left(\Phi_{UT,n} + \Phi_{BT,n}\right). \tag{2.44}$$

Taking into account Eqn. (2.44) along with Eqns. (2.42) and (2.40) yields:

$$\Delta\Phi = \frac{\Phi_0(1-R)\left(1-e^{-\alpha b}\right)}{1-Re^{-\alpha b}} \tag{2.45}$$

Next, we wish to investigate the total photon flux density and photon absorption rate in a layer of thickness Δx situated at depth x below the illuminated surface as shown in Figure 2.11. The photon flux density entering the layer through the top surface after n^{th} order is given by:

$$\Phi_{ui,n} = \Phi_0(1-R)^2 R^{2n} e^{-\alpha(2nb+x)}, \qquad (n = 0, 1, 2, 3 \dots). \tag{2.46}$$

The photon flux density leaving the layer through the top surface after n^{th} order is given by:

$$\Phi_{ut,n} = \Phi_0(1-R) R^{(2n-1)} e^{-\alpha(2nb-x)}, \qquad (n = 1, 2, 3 \dots). \tag{2.47}$$

The photon flux density entering the layer through the bottom surface after n^{th} order:

$$\Phi_{bi,n} = \Phi_0(1-R) R^{(2n-1)} e^{-\alpha(2nb-x-\Delta x)}, \qquad (n = 1, 2, 3 \dots). \tag{2.48}$$

The photon flux density leaving the layer through the bottom surface after n^{th} order:

$$\Phi_{bt,n} = \Phi_0(1-R)^2 R^{2n} e^{-\alpha(2nb+x+\Delta x)}, \qquad (n = 0, 1, 2, 3 \dots). \tag{2.49}$$

The total photon flux density absorbed in the layer of thickness Δx is given by:

$$\Delta\Phi(\alpha, x, \Delta x) = \sum_{n=0}^{\infty} \left(\Phi_{ui,n} - \Phi_{bt,n}\right) + \sum_{n=1}^{\infty} \left(\Phi_{bi,n} - \Phi_{ut,n}\right). \tag{2.50}$$

Substitution of Eqns.(2.46) to (2.49) into Eqn.(2.50) gives:

$$\Delta\Phi(\alpha, x, \Delta x) = \frac{\Phi_0(1-R)e^{-\alpha x}\left(1-e^{-\alpha\Delta x}\right)\left(1+Re^{-\alpha(2(b-x)-\Delta x)}\right)}{1-R^2 e^{-2\alpha b}}. \tag{2.51}$$

The photon absorption rate in this layer is hence described by dividing Eqn.(2.51) by Δx as:

$$g_0(\alpha, x, \Delta x) = \frac{\Phi_0(1-R)e^{-\alpha x}(1-e^{-\alpha\Delta x})\left(1+Re^{-\alpha(2(b-x)-\Delta x)}\right)}{\Delta x(1-R^2e^{-2\alpha b})}. \quad (2.52)$$

Next, we are going to investigate the effect of photon generation rate in each layer of a thin film of semiconductor. Consider a sample of thin film of thickness b with depletion layers of equal thicknesses b_1 on either sides under the two surfaces. We assumed the presence of highly depleted layers and transition layers of thicknesses b_S and b_δ, respectively in both depletion layers. The photon absorption rate in the highly depleted layer under the illuminated surface is determined by putting $x = 0$ and $\Delta x = b_S$ as:

$$g_{0S}(\alpha, b_S) = \frac{\Phi_0(1-R)(1-e^{-\alpha b_S})\left(1+Re^{-\alpha(2b-b_S)}\right)}{b_S(1-R^2e^{-2\alpha b})}. \quad (2.53)$$

For the transition layer under the illuminated surface is determined by putting $x = b_S$ and $\Delta x = b_\delta$ as:

$$g_{0\delta}(\alpha, b_S, b_\delta) = \frac{\Phi_0(1-R)e^{-\alpha b_S}(1-e^{-\alpha b_\delta})\left(1+Re^{-\alpha\left(2b-(b_S+b_1)\right)}\right)}{b_\delta(1-R^2e^{-2\alpha b})}. \quad (2.54)$$

For the quasi-neutral region it is determined by putting $x = b_1$ and $\Delta x = b - 2b_1$ as:

$$g_0(\alpha, b_1, b-2b_1) = \frac{\Phi_0(1-R)e^{-\alpha b_1}\left(1-e^{-\alpha(b-2b_1)}\right)}{(b-2b_1)(1-Re^{-\alpha b})}. \quad (2.55)$$

For the transition layer under the bottom surface is determined by putting $x = b - b_1$ and $\Delta x = b_\delta$ as:

$$g_{0\delta}(\alpha, b-b_1, b_\delta) = \frac{\Phi_0(1-R)e^{-\alpha(b-b_1)}(1-e^{-\alpha b_\delta})\left(1+Re^{-\alpha(b_1+b_S)}\right)}{b_\delta(1-R^2e^{-2\alpha b})}. \quad (2.56)$$

For the highly depleted layer under the surface is determined by putting $x = b - b_S$ and $\Delta x = b_S$ as:

$$g_{0S}(\alpha, b-b_S, b_S) = \frac{\Phi_0(1-R)e^{-\alpha(b-b_S)}(1-e^{-\alpha b_S})(1+Re^{-\alpha b_S})}{b_S(1-R^2e^{-2\alpha b})}. \quad (2.57)$$

To find the photon absorption rate at a point situated x distance below the illuminated surface, we make $\Delta x \to 0$, and hence, one can consider the approximation $1 - e^{-\alpha \Delta x} \approx \alpha \Delta x$ and $b \pm \Delta x \approx b$ in Eqn. (2.52) above, so that:

$$g_0(\alpha, x) = \frac{\Phi_0 \alpha (1-R) e^{-\alpha x}\left(1 + R e^{-2\alpha (b-x)}\right)}{1 - R^2 e^{-2\alpha b}}. \tag{2.58}$$

Under the illuminated surface, $x \to 0$ and hence

$$g_0(\alpha) = \frac{\Phi_0 \alpha (1-R)(1 + R e^{-2\alpha b})}{1 - R^2 e^{-2\alpha b}}. \tag{2.59}$$

Near the bottom surface, $x \to b$ and

$$g_0(\alpha, x) = \frac{\Phi_0 \alpha (1-R^2) e^{-\alpha b}}{1 - R^2 e^{-2\alpha b}}. \tag{2.60}$$

The total photon absorption rate in the entire sample of thickness b can be determined from Eqn. (2.52) by changing Δx to the sample thickness b and taking the depth to the surface ($x \to 0$) as:

$$G_0(\alpha, b) = \frac{\Phi_0 (1-R)\left(1 - e^{-b/x_p}\right)}{b\left(1 - R e^{-b/x_p}\right)}, \qquad \alpha = \frac{1}{x_p}. \tag{2.61}$$

The limiting values of the total photon absorption rate in Eqn. (2.61) can be generalized as:

$$G_0(\alpha, b) = \begin{cases} \Phi_0 \alpha, & \text{for } b \ll x_p, \\ \dfrac{0.63 \Phi_0 (1-R)}{b(1 - 0.37R)}, & \text{for } b = x_p, \\ \dfrac{\Phi_0 (1-R)}{b}, & \text{for } b \gg x_p. \end{cases} \tag{2.62}$$

2.6.3 Optical Generation and Recombination of excess carriers

2.6.3.1 Generation/recombination rate equation

The rates of change of electrons in the conduction band and holes in the valence band are equal and always given by the difference between the generation and the recombination rates, *i.e.*:

$$\frac{dn}{dt} = \frac{dp}{dt} = G - R. \tag{2.63}$$

where n and p represent the non-thermal equilibrium electron and hole concentrations in the conduction and valence bands respectively, and G and R are the total generation and recombination rates of charge carriers, respectively. The total generation rate involves both the thermal (G_{th}) and optical (G_0) generation rates:

$$G = G_{th} + G_0. \tag{2.64}$$

The net excess carrier recombination rate U is defined as the difference between the total recombination rate and the thermal equilibrium generation rate:

$$U = R - G_{th}. \tag{2.65}$$

The net recombination rates for photo-generated electrons and holes are given by:

$$U = \frac{\delta n}{\tau_n} = \frac{\delta p}{\tau_p}. \tag{2.66}$$

where δn and δp are the concentrations of photo-generated carriers. The parameters τ_n and τ_p are called the electron and hole recombination lifetimes, respectively. Using the principle of detailed balance along with Eqns. (2.63) to (2.66), the rates of change of the excess carriers are:

$$\frac{d\delta n}{dt} = G_0 - U = \frac{d\delta p}{dt}. \tag{2.67}$$

Electron-hole pairs are continuously generated under illumination, and the excess charge carrier concentrations will increase. Recombination, on the other hand, tries to reduce the excess carrier concentrations to zero.

2.6.3.2 Recombination mechanism in semiconductors

Generation in semiconductors refers to the process by which electron-hole pairs are created. The electron–hole pair is the fundamental unit of generation and recombination, corresponding to an electron transition between the valence band and the conduction band. Recombination refers to the inverse processes by which the electron-hole pairs are lost due to the spontaneous transition of an excited electron from conduction band to a hole in valence band. The annihilation of excess carriers generated by electrical in a semiconductor

may take place via different recombination mechanisms [42]. Once the electron-hole pairs are generated by absorption in the semiconductor, they are exposed to several recombination mechanisms.

Depending on the ways in which the energy of an excess carrier is removed during a recombination process, there are different basic recombination mechanisms, which are responsible for carrier annihilation in a semiconductor [43]. But, in the next section we are going to investigate only the radiative recombination mechanisms and the lifetime associated with it for a small band gap of a p-type semiconductor.

1. Radiative Recombination

Radiative recombination is the direct annihilation of an electron-hole pair. Band-to-band radiative recombination in a semiconductor is the inverse process of optical absorption. The excess energy is being released mainly as a photon with energy close to that of the band gap. In the radiative recombination, the energy of an electron is given as a photon during recombination [44]. Emission of photons as a result of band-to-band radiative recombination is common in a direct band gap semiconductor. In a nondegenerate semiconductor, the rate at which electrons and holes are annihilated via band-to-band radiative recombination is proportional to the product of electron and hole densities in the conduction and valence bands, respectively. In thermal equilibrium, the rate of band-to-band recombination is equal to the rate of thermal generation, which can be expressed by:

$$R_0 = c_R n_0 p_0 \ . \tag{2.68}$$

where n_0 and p_0 are the thermal equilibrium electron and hole densities respectively and c_R is a constant known as the coefficient of holes in the valence band for the capture of electrons, and is related to the electron capture cross-section (σ_R) and the thermal velocity of the electrons (v_{th}) [45, 46]:

$$c_R = \sigma_R v_{th}. \tag{2.69}$$

The capture cross-section can be thought of as the volume swept out per unit time by a particle. When the dispersion in the dielectric constant is ignored, the band-to-band capture coefficient for bands with spherical symmetry was shown by van Roosbroeck and Shockley to depend on the absorption coefficient through the relation [47]:

$$C_R = \frac{8\pi k_\infty}{c^2} \int_0^\infty \frac{\alpha(\upsilon)\upsilon^2 d\upsilon}{\exp\left(\frac{h\upsilon}{k_B T}\right) - 1} \ , \tag{2.70}$$

The radiative recombination coefficient C_R has a value of $2 \times 10^{-10} cm^{-3} s^{-1}$ at 300 K as calculated using the expression derived by Van Roosbroeck and Shockley. The values of C_R can be obtained by numerical integration of Eqn.(2.70) for narrow band gap semiconductors as [33]:

$$C_R = e\pi\sqrt{k_\infty}\left(\frac{m_n}{m_n^* + m_p^*}\frac{300}{T}\right)^{\frac{3}{2}}\left(1 + \frac{m_n}{m_n^*} + \frac{m_n}{m_p^*}\right)\left[E_g^2 + 3E_g k_B T + 3.75 k_B^2 T^2\right], \tag{2.71}$$

where E_g and $k_B T$ are in electron volt (eV).

Under steady-state conditions, the rate of band-to-band radiative recombination is given by:

$$R = c_R np. \tag{2.72}$$

where $n = n_0 + \delta n$ and $p = p_0 + \delta p$. The net recombination rate is obtained by solving Eqns.(2.68) and (2.72) and resulting in:

$$\mathrm{U_R} = c_R(\mathrm{np} - n_i^2). \tag{2.73}$$

In the radiative recombination, electron hole pairs recombine directly from band to band with the energy carried away by photons. The concepts of carrier lifetime in semiconductor materials and average life expectancy in demography are similar. Like common mortals, electrons (and holes) die after some time and the average of this time is called the minority carrier lifetime [46].

The excess carrier lifetimes under steady-state conditions are defined by the ratio of the excess carrier density and the net capture rate for electrons and holes, and are given respectively by [48]:

$$\tau_n = \frac{\delta n}{U_n} \ , \qquad \text{for electrons} \tag{2.74}$$

$$\tau_p = \frac{\delta p}{U_p}, \qquad \text{for holes} \tag{2.75}$$

For the small injection case (i.e., $\delta n \ll n_0$ and $\delta p \ll p_0$), the charge-neutrality condition requires that:

$$\delta n = \delta p \, . \tag{2.76}$$

The radiative lifetime (τ_R) due to the band-to-band recombination is obtained by solving Eqns.(2.73) and (2.76), which yields:

$$\tau_R = \frac{\delta n}{U_r} = \frac{1}{c_R(p_0 + n_0 + \delta n)}, \tag{2.77}$$

From Eqn. (2.77) , it is noted that τ_R is inversely proportional to the majority carrier density. Under low injection level, Eqn. (2.77) can be simplified to:

$$\tau_R = \tau_{R0} = \frac{1}{c_R(p_0 + n_0)}, \tag{2.78}$$

Using Eqns. (2.73) , (2.67) and (2.78), one can determine the rate of excess free carrier accumulation:

$$\frac{d\delta n}{dt} = G_0 - \left(\frac{\delta n}{\tau_{R0}} + C_R \delta n^2\right) \tag{2.79}$$

The steady-state solution of Eqn.(2.79) is:

$$\delta n = \frac{2G_0 \tau_k \tau_{R0}}{\tau_{R0} + \tau_k}. \tag{2.80}$$

and

$$\tau_R = \tau_g = \frac{2\tau_k \tau_{R0}}{\tau_{R0} + \tau_k}, \tag{2.81}$$

where τ_k is the time constant given by:

$$\tau_k = \frac{\tau_{R0}}{\sqrt{1 + 4C_R G_0 \tau_{R0}^2}}. \tag{2.82}$$

2. Effective excess carrier lifetime in thin films

The performance of a semiconductor material depends on the lifetime of free charge carriers generated by the interaction of light with the material, referred to as the excess

carrier lifetime (τ). The excess carrier lifetime is in general determined by the recombination rate of the minority charge carriers at the surface and in the bulk of the material.

For a steady state condition, the excess carrier generation rate (G_0) is equal to their reverse recombination rate (R). The photo-generated carrier concentration ($\Delta\delta$) in the entire sample is proportional to the product of both the recombination or generation rate and the excess carrier lifetime. Thus, the free carriers' generation rate is affected by the photon flux density, energy of the illumination and thickness of the sample. Hence, the photo-generated carrier concentration ($\Delta\delta$) in the entire sample is given as:

$$\delta n = G_0 \tau_{\text{eff}}. \tag{2.83}$$

The absorbed photons create excess electron–hole pairs and as a result the densities of electrons and holes increase above their equilibrium value. This also results in the increment of the conductivity of the material. This increment in the conductivity of the material due to illumination by light is called photoconductivity of the material [33]. Thus, the change in the sample conductivity due to illumination is given by:

$$\delta\sigma = e(\mu_n + \mu_p)\mathrm{G}_0\tau_{\text{eff}}, \tag{2.84}$$

where e is the elemental charge, μ_n and μ_p are the electron and hole mobilities, respectively. The effective excess minority carrier lifetime in the entire sample (*i.e.* bulk plus surface recombination) is determined by considering the sum of the recombination rates through the sample. The radiative recombination mechanisms discussed so far may occur in a given semiconductor material. The average (mean) radiative excess carrier lifetime in the entire sample denoted by τ_{eff} can be calculated using the relation [49]:

$$\tau_{\text{eff}} = \frac{1}{b}\int_0^b \tau_R(x)dx, \tag{2.85}$$

where b is the thickness of the sample.

Chapter 3

Methodology

The primary task of this work was to select the model of a pure direct band semiconductor sample in which band to band transition is most effective. Gallium antimonide (GaSb) was found to be suitable for its small and direct bandgap and its very high purity. The majority carrier concentration, p_0 used in the analysis for different doping levels GaSb samples was taken from the simulation of the existing temperature dependence Hall measurements data measured at Nelson Mandela Metropolitan University, South Africa. The minority carrier concentration, n_0 is determined from p_0 and the intrinsic carrier concentration using the law of mass action for a particular semiconductor using the relation in Eqn. (2.16).

Then, the photon absorption rate in the bulk semiconductor is described using the technique discussed in Section 2.6.1. Bulk semiconductor was modelled to determine photon absorption effect in different layers of bulk semiconductor. The model of bulk semiconductor most used was illustrated in Figure 2.10. By using illumination mechanisms the total absorbed photon flux density, the penetration depth (x_p) of a photon in a semiconductor, the photon absorption rate at the surface and in the bulk of a very thick semiconductors were studied in details and the photon absorption rate at a point at depth x below the illuminated surface in very thick semiconductor were determined from the relation in Eqn. (2.33). At thin film semiconductor was also modelled to determine photon absorption effect in different layers of thin film semiconductor. The model of thin film semiconductor most used was illustrated in Figure 2.11. By using illumination mechanisms, the total photon flux density and photon absorption rate in a layer of thickness Δx situated at depth x below the illuminated surface were investigated in details. By taking a sample of thin film of thickness b with depletion layers of equal thicknesses b_1 on either sides under the two surfaces, the photon generation rate effect in each layer of a thin film of semiconductor are also determined. Moreover, the photon absorption rate at a point situated x distance below the illuminated surface and the total photon absorption rate in the entire sample of thickness b were described using Eqns. (2.58) and (2.61), respectively. In the analysis of this result, the

vertical axis for the photon absorption rate and horizontal axis of the absorption coefficient and depth below the surface was taken as semi-log for both thin film and thick film semiconductor.

By using the steady-state radiative recombination mechanism for small band gap of a p-type semiconductor, the expression for the radiative excess carrier lifetime was obtained in terms of the doping level, the injection level and absorption coefficient at different depths of the material. The effects of doping level, injection level and the energy of the illumination on the photo-response of the material at different depths below the illuminated surface are investigated in detail. Finally, the average (mean) radiative excess carrier lifetimes were investigated as function of depth and thickness of the samples in different samples.

Chapter 4

Analysis of data and Discussions

This chapter presents the analysis and discussion of the entire results of this work. First, the photon absorption rate in both the bulk and thin films semiconductors were presented and compared. Then, the comparison of the photo-response (radiative excess carrier lifetime) for both bulk and thin films semiconductors were continued. The method can also be applied for the determination of Auger excess minority carrier lifetime for a small band gap of Gallium antimonide (GaSb) semiconductor. Nevertheless, since the variation of the impact ionization is similar to the radiative effect except the variation in the magnitude in the two cases, we wish to limit the analysis only to the radiative excess carrier lifetime.

4.1 Photon absorption rate in both bulk and thin film semiconductor

4.1.1 At different depths and Absorption coefficients

The photon absorption rate in this case is obtained as a function of absorption coefficient (α) and depth (x) below the illuminated surface of the sample using Eqns. (2.33) and (2.58) for the bulk and thin films, respectively. Figure 4.1 illustrates the photon absorption rate in the entire sample as a function of (a) absorption coefficient for samples with different thicknesses and (b) depths below the surface for photons with different absorption coefficients in the bulk of the sample. As one can see from the two figures, photons with higher absorption coefficients (energies) are absorbed more near the illuminated surface and photons with very low absorption coefficients (energies) are passing through the materials without being absorbed (or with a few absorption effect). As it can be seen from Figure 4.1 (a), the value of the absorption rate at each depth goes to zero for very large and small value of α and has maximum absorption rate pick of $\Phi_0\alpha(1-R)\exp(-1)$ at the value of x equal to the reciprocal of α. This clearly shows that, when a point at a depth, x below the illuminated surface is illuminated by photons of different energy, only a photon with α equal to the reciprocal of x has relatively very large absorption rate of $\Phi_0\alpha(1-R)\exp(-1)$ as compared to other photons with more or less energies. The values of the absorption rate each photon can have at any depth is indicated by blue lines in the semi log graphs of Figure 4.1 (a) and (b). As can be seen from Figure 4.1 (b) (see brown lines), each photon has a

maximum absorption rate of $\Phi_0\alpha(1-R)$ at the illuminated surface of the bulk material and the value of the absorption rate diminishes with increasing the depth below the illuminated surface. The absorption rate also decreases to $\Phi_0\alpha(1-R)\exp(-1)$ at $x = 1/\alpha$, which is equal to the penetration depth of this particular photon in the material.

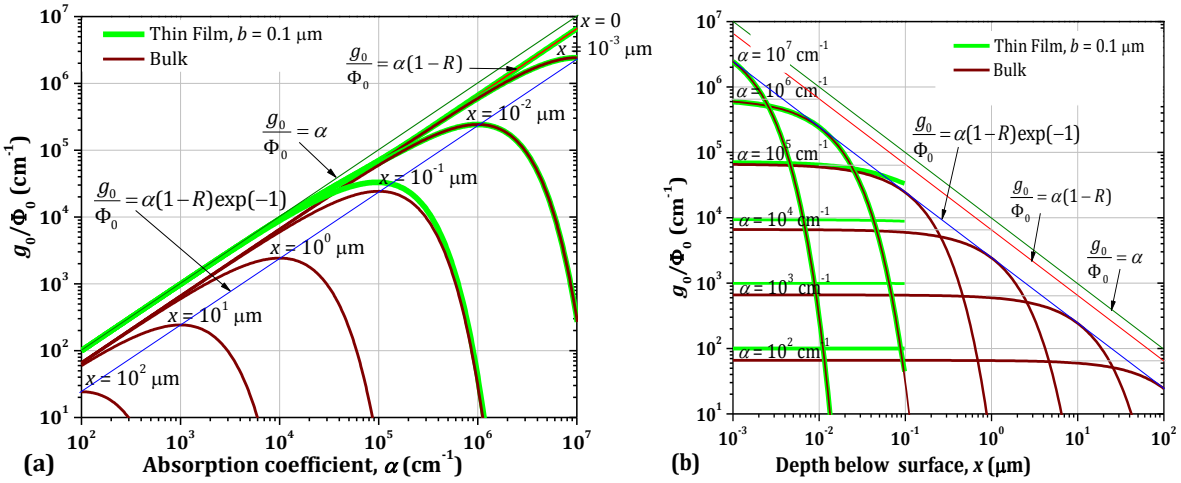

Figure 4.1: Comparison of photon absorption rate in both thin film and bulk (thick) semiconductor as a function of (a) absorption coefficient for different depths in the sample (x) and (b) as a function of depth below the surface for photons with different absorption coefficients ($R = 0.34,\ b = 0.1\mu m$).

The distinctive behavior of thick (bulk) and thin film semiconductors in this case is that, in thick semiconductor, if a photon of flux density, Φ_0 is illuminating the surface, the amount $\Phi_0 R$ is reflected back and the absorption rate at depth x below the illuminated surface is given by Eqn. (2.33). Hence, the maximum absorption rate of $\Phi_0\alpha(1-R)$ occur just under the illuminated surface as shown by red lines in both Figure 4.1 (a) and (b). Whereas, the absorption rate at depth x below the illuminated surface in thin film semiconductors which is described using relation in Eqn. (2.58) gives a maximum of photon flux density $\Phi_0\alpha$ under the illuminated surface of thin film. This indicates that, the reflection effect is compensated in thin films due to the multiple reflections of photon from the top and the bottom surfaces into the film. As a result, each point inside a thin film semiconductor has more photon absorption rates as compared to the corresponding points in thick semiconductors. This phenomenon is illustrated in Figure 4.1 (a) and (b) using brown curves, green lines and curves. The brown curve shows the effects of absorption rate at depth x below the illuminated in thick semiconductor that has maximum value $\Phi_0\alpha(1-R)$ just under the illuminate surface. The green curve shows the effects of absorption rate at depth x below the illuminated in very thin film semiconductor that has maximum value $\Phi_0\alpha$ just under the

illuminated surface. The photon absorption rate in Figure 4.1 (a) and (b) has in general three limiting values. These are, the maximum absorption rate just under the surface of a thin film represented by the green line, the maximum absorption rate just under the surface of a thick material represented by the red line and the absorption rate at the absorption depth under the illuminated surface of a thick material represented by the blue line.

4.1.2 For different thicknesses of samples and Absorption coefficients

Figure 4.2 illustrates the total photon absorption rate in both thin film and bulk semiconductor as (a) a function of absorption coefficient for different thicknesses of the samples (b) function of thickness for different absorption coefficients. The analysis of this data is performed using Eqn. (2.61) that describes the general expression of the total photon absorption rate in terms of the absorption coefficient and the thickness of the material. The bulk semiconductor corresponds to a material with very large thickness and thin film corresponds to materials with very small thickness ($b < 1/\alpha$).

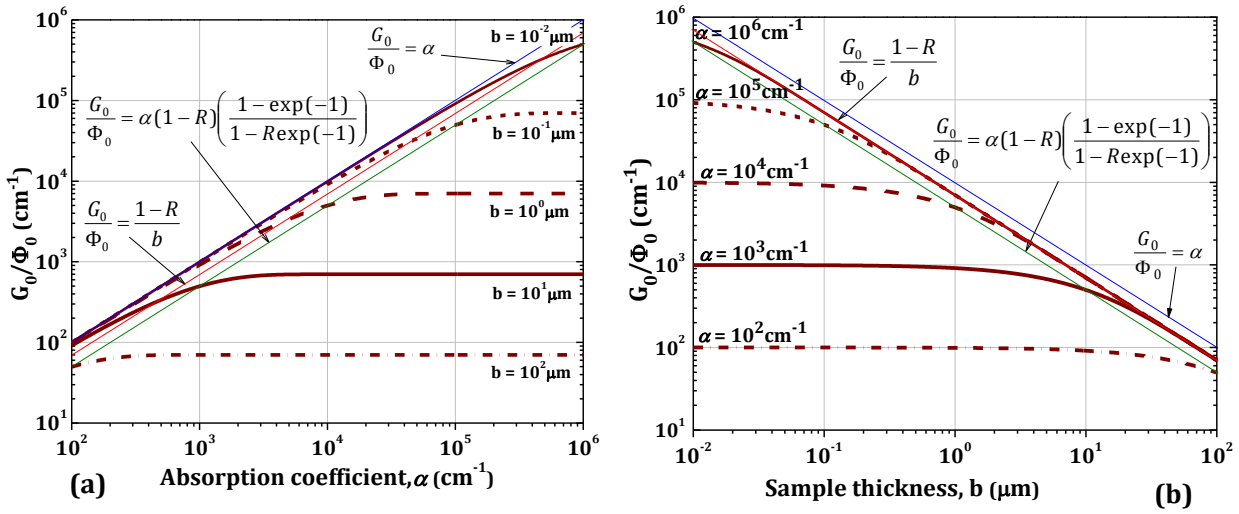

Figure 4.2: Total photon absorption rate in both thin film and bulk semiconductor as (a) function of absorption coefficient for different thicknesses of the samples (b) function of thickness for different absorption coefficients.

The total photon absorption rate in Figure 4.2 (a) and (b) has also three limiting values. These are, the maximum photon absorption rate in very thin film ($b < 1/\alpha$) represented by the blue line, the maximum photon absorption rate when the thickness of the material is equal to the penetration depth of the corresponding photon ($b = 1/\alpha$), represented by the green line and the photon absorption rate when the thickness of the material is greater than

the penetration depth of the corresponding photon ($b > 1/\alpha$), represented by the red line. The effects of the variation of the photon absorption rate with absorption coefficient and thickness of the samples is easily understandable when explained using the illustrations like Figure 4.2 (a) and (b). Both of these figures describe that, photons with very high energies are absorbed at very high rate in very thin films and photons with very low energy are passing unabsorbed (with less absorption) through the materials.

Figure 4.2 (a), also reveals that, the variation of the absorption rate with the energy of the illumination is very high in thin films than in thick materials of semiconductors. That is, different photons are absorbed with the same rate in a thick film, but they are absorbed with different rates in thin films. The rate of absorption is increasing with decreasing thickness. Figure 4.2 (b) also shows that, the variation of the absorption rate with the thicknesses of the samples is very high for high energy photons. That means, a low energy photon can be absorbed with a constant rate in very thin films of different thicknesses, but is absorbed with different rates in thick films. The absorption rate increases with increasing the energy of illumination.

4.2 Determination of Radiative excess carrier lifetime as a function of depth at different doping levels

4.2.1 Low injection level and Low energy consideration

The photo-response of a semiconductor also depends on the doping level, the injection level of the photon flux density, the energy of the illumination, the thickness of the material and the depth of the point under consideration below the illuminated surface. As already discussed in the literature part, the layer under the surface of GaSb is depleted of majority charge carriers and has very low thermal equilibrium majority carriers as compared to the deep bulk. Hence, the recombination rate of photo-generated free carriers is relatively very small in this region as compared to the deep bulk. This enhances the magnitude of the excess carrier lifetime in the under surface depletion layer than in the deep bulk.

For the description of photo-response of the material under low injection level, the data of the radiative excess minority carrier lifetime is obtained by using Eqns. (2.77) to (2.85). First, the low level injection radiative excess minority carrier lifetime is determined as a function of the depth below the illuminated surface for four samples with different doping

levels $1.8 \times 10^{16}\text{cm}^{-3}$, $1.8 \times 10^{17}\text{cm}^{-3}$, $1.8 \times 10^{18}\text{cm}^{-3}$, and $1.8 \times 10^{19}\text{cm}^{-3}$ by keeping the energy and the photon flux density at their possible lowest values. The typical value of the room temperature radiative capture coefficient for GaSb used in this analysis is $2 \times 10^{-10}\ \text{cm}^{-3}\text{s}^{-1}$.

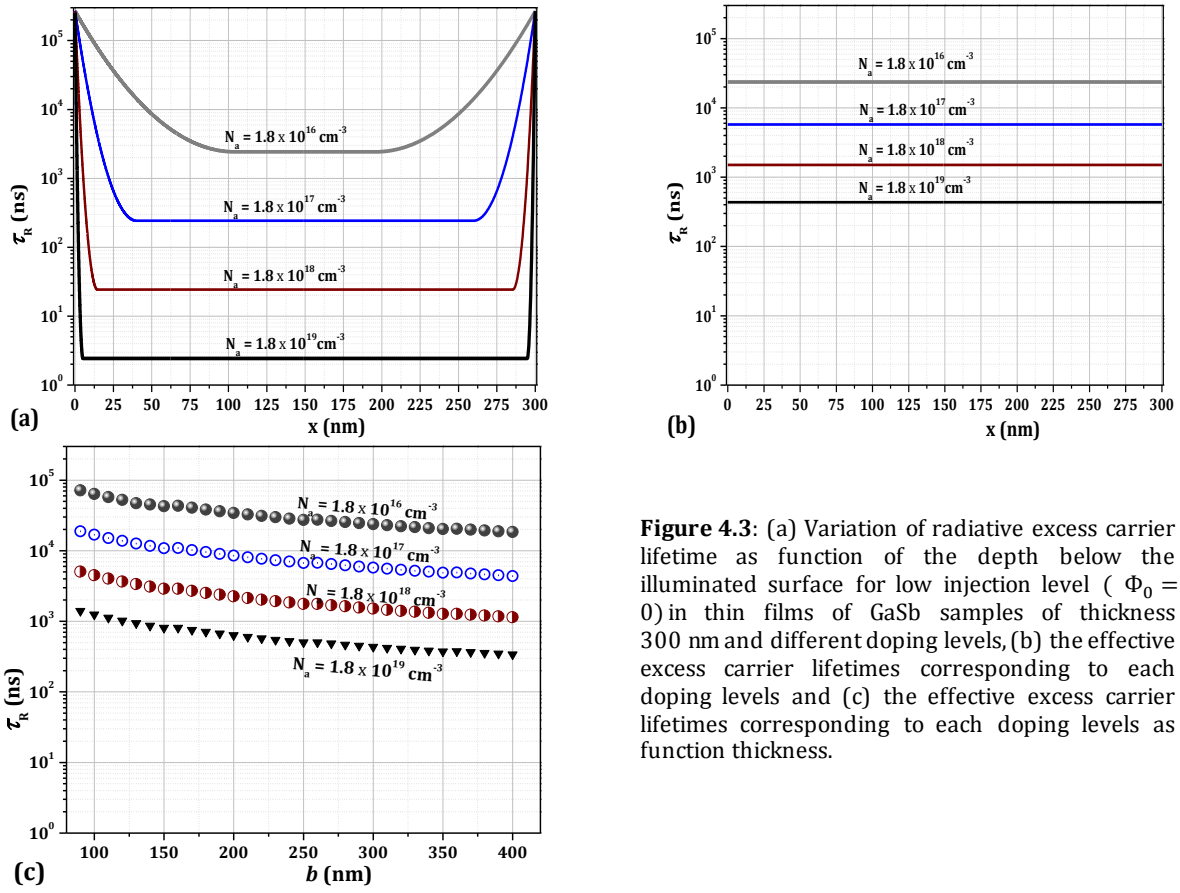

Figure 4.3: (a) Variation of radiative excess carrier lifetime as function of the depth below the illuminated surface for low injection level ($\Phi_0 = 0$) in thin films of GaSb samples of thickness 300 nm and different doping levels, (b) the effective excess carrier lifetimes corresponding to each doping levels and (c) the effective excess carrier lifetimes corresponding to each doping levels as function thickness.

Figure 4.3 depicts (a) the variation of radiative excess carrier lifetime as function of the depth below the illuminated surface for low injection level ($\Phi_0 = 0$) in thin films of GaSb samples of thickness 300 nm and different doping levels, (b) the effective excess carrier lifetimes corresponding to each doping levels and (c) the effective excess carrier lifetimes corresponding to each doping levels as function thickness. Figure 4.3 (a) illustrates that; the magnitude of the radiative excess minority carrier lifetime is highly decreasing in the deep bulk of the semiconductor with increasing the doping level, while the magnitude of the radiative excess minority carrier lifetime under the surface is insensitive to the doping level. This is an evidence that the surface property is unaltered by the doping effect of the material

and the surface Fermi level position is pinned regardless of the doping level of the sample [50] . The radiative excess carrier lifetime is 400 ns at doping level of $1.8 \times 10^{17} cm^{-3}$ in the deep bulk of the semiconductor. The results obtained in this work is comparable with the result reported by R. N. Hall which is 0.37μs at doping level of $10^{17} cm^{-3}$ in the deep bulk of GaSb [51]. A large range of values for the carrier lifetime of GaSb has been reported. Titkov et al. observed photoelectron lifetimes of a few nanoseconds for heavily doped p-type GaSb [32].

The difference between the surface and the deep bulk photo-response is also highly exaggerated with increasing the doping level. This is because the majority carrier concentration in the depletion layer decreases from maximum value p_0 at the edge of the quasi-neutral region towards the surface and attains its minimum value at the surface. As a result, the surface contributes very high mean minority carrier lifetime obtained using Eqn. (2.85) in the entire semiconductor as depicted in Figure 4.3 (b) and (c) as function of depth and thickness, respectively. Even though, the mean minority carrier lifetime in the entire sample shown in Figure 4.3 (b) and (c) decreases with increasing the doping level, the difference between the bulk excess carrier lifetime and the mean minority carrier lifetime increases with increasing the doping level. Therefore, the role of the surface depletion layer in the photo-response of the material is very essential in highly doped samples where the bulk is insensitive to the illuminations.

4.2.2 Single doping, different injection levels and absorption coefficients consideration

Figure 4.4 illustrates variation of radiative excess minority carrier lifetimes with depth below the illuminated surface for (a) different injection and low absorption coefficient, (b) different injection and high absorption coefficient and (c) high injection level and different absorption coefficients for GaSb thin film of doping level 6.83×10^{16} cm^{-3} and thickness 300 nm. In Figure 4.4 (a), the absorption coefficient is kept at very low value of 10^{-3} cm^{-1} and the photon flux density injection level is varied from 0 to 10^{32} $cm^{-2}s^{-1}$. The surface remains under high injection for all the illuminations except at 0 photon flux density, while the deep bulk is under high injection level only for the three high injection level illuminations with photon flux densities 10^{27} $cm^{-2}s^{-1}$, 10^{29} $cm^{-2}s^{-1}$ and 10^{32} $cm^{-2}s^{-1}$. Since a photon with

low energy can pass through a thin material with a constant low absorption rate as discussed in Figure 4.1 (b), equal amounts of free carrier concentrations, δn are generated by the illumination at all depths inside the material.

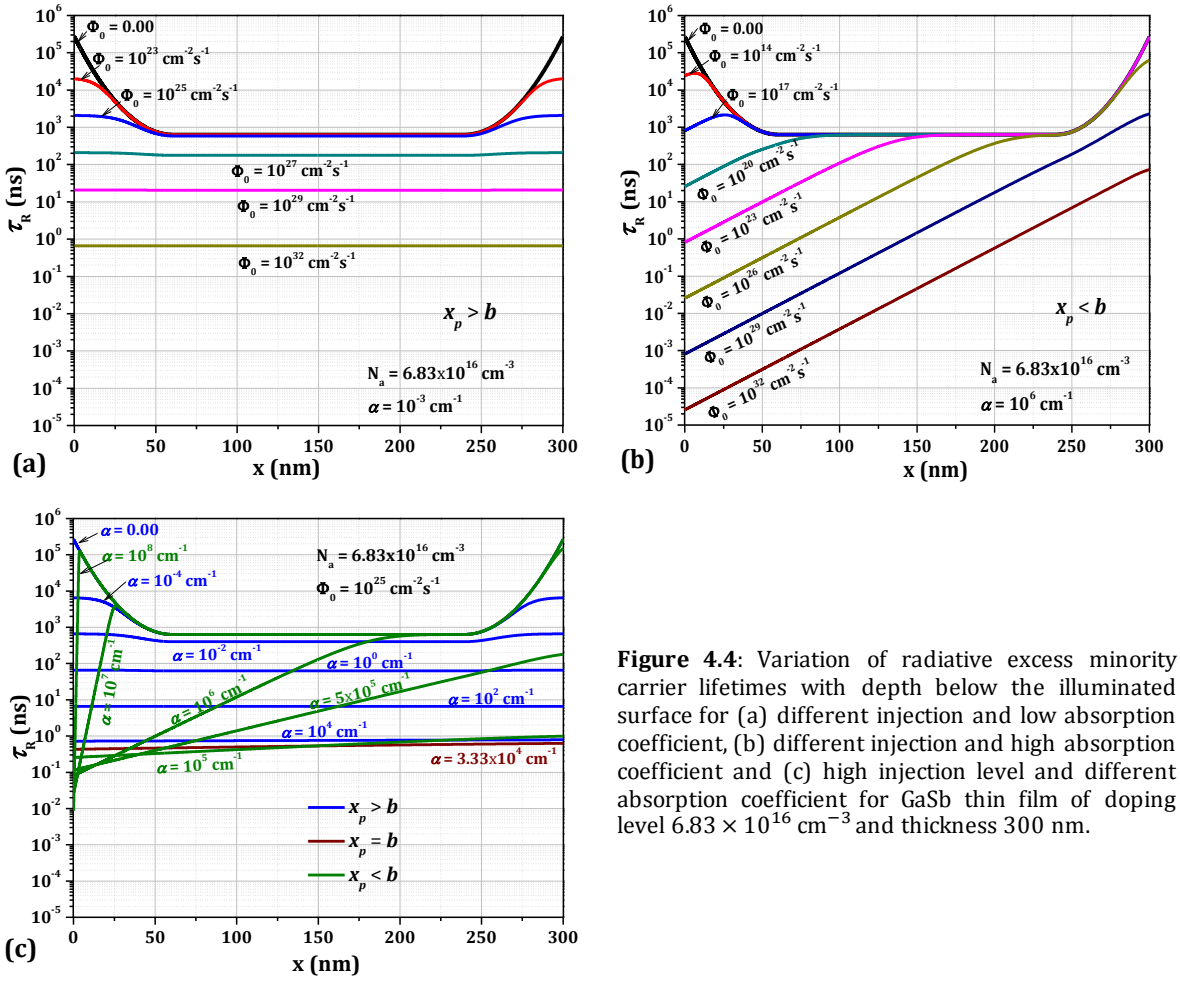

Figure 4.4: Variation of radiative excess minority carrier lifetimes with depth below the illuminated surface for (a) different injection and low absorption coefficient, (b) different injection and high absorption coefficient and (c) high injection level and different absorption coefficient for GaSb thin film of doping level 6.83×10^{16} cm^{-3} and thickness 300 nm.

Since the under surface regions have very low thermal equilibrium majority carrier concentration, p_{0S}, they always remain under high injection level condition under the situations where $p_{0S} < \delta n$, while the deep bulk with very high thermal equilibrium majority carrier concentration, p_0 (or $p_0 > \delta n$) still remains under low injection level as depicted by the two low injection levels 10^{23} cm^{-2}s^{-1} and 10^{25} cm^{-2}s^{-1} in Figure 4.4 (a). The photo-response of the surface region is higher than the bulk in this case. With increasing the injection level of the photon flux density that can generate free carriers concentration more than the thermal equilibrium carrier concentrations in the bulk (or $p_0 < \delta n$) as indicated by the three higher injection levels 10^{27} cm^{-2}s^{-1}, 10^{29} cm^{-2}s^{-1} and 10^{32} cm^{-2}s^{-1}, both the under surface layers and the deep bulk layers remain under the same high injection levels.

Hence, the effects of high injection level and low energy photons can be detected equally at all points inside a thin film material, while the effects of the low injection level and low energy photons cannot be detected in the deep bulk, but can be detected under the top and the bottom surfaces as illustrated in the upper part of Figure 4.4 (a). The excess carrier lifetime also decreases with increasing the injection level.

In Figure 4.4 (b), the absorption coefficient is kept at very high value of 10^6 cm^{-1} and the photon flux density injection level is varied from 0 to 10^{32} $\text{cm}^{-2}\text{s}^{-1}$ as in Figure 4.4 (a). Again, the surface remains under high injection for all the illuminations except at 0 photon flux density, while the deep bulk is under low injection level only for the two low injection level illuminations with photon flux densities 10^{14} $\text{cm}^{-2}\text{s}^{-1}$ and 10^{17} $\text{cm}^{-2}\text{s}^{-1}$. The effects of these two injection levels cannot be detected in the deep bulk and under the bottom surface.

Since the absorption rate of a photon with high energy is very high closer to the illuminated surface and decreases with increasing the depth below the illuminated surface as already discussed in detail in Figure 4.1 (b), more amounts of free carrier concentrations, δn are generated by the illumination closer to the illuminated surface and this effect decreases with increasing the depth from the illuminated surface, so that the region under the bottom surface has minimum free carrier concentration. The under surface regions still remain under high injection level condition for $p_{0S} < \delta n$, while the deep bulk with very high thermal equilibrium majority carrier concentration, p_0 shows different response at different positions to all the injection levels with the same higher photon energy. Due to the presence of maximum free carrier concentration under the illuminated surface, the excess carrier lifetime also has minimum value here as compared to the other points inside the material. The value of the excess carrier lifetime corresponding to each injection level also increases with increasing the depth below the illuminated surface and attains maximum value under the bottom surface where the free carrier's concentration is relatively very low. Hence, the effect of an illumination with high energy and high injection level can be detected at different points inside a material with various photo-responses. However, the effect of an illumination with high energy and low injection level can be detected only under the illuminated surface as shown in Figure 4.4 (b).

In Figure 4.4 (c), the illumination photon flux density is kept at very high value of 10^{25} $cm^{-2}s^{-1}$ and the absorption coefficient is varied from 0 to 10^{8} cm^{-1}. The low energy photons with $b < 1/\alpha$ (blue lines) generate free carriers at the same rate at all points inside the material, so that the photo-response of the materials to these photons remains uniform. Nevertheless, when the penetration depth of the photon becomes equal to the thickness of the film ($b = 1/\alpha$), the absorption rate under the bottom surface reaches its maximum value as discussed in Figure 4.1 (a). This gives a possible minimum excess carrier lifetime under the bottom surface represented by a brown line with $\alpha = 1/b = 3.33 \times 10^{4}$ cm^{-1}. Photons with energies more than this limit ($b > 1/\alpha$) cannot reach the bottom surface and mainly absorbed closer to the top surface and show similar to the one discussed in Figure 4.1 (b). That is, for very high energy illumination, the free carrier's generation rate under the illuminated surface increases with increasing the absorption rate and that in the deep bulk and under the bottom surface decrease with increasing the absorption coefficient, α. All the green lines shown in Figure 4.1 (c) are the photo-responses of photons with $b > 1/\alpha$. Note that, the slopes of the lines increase with increasing α. Therefore, one can conclude from this result also that, the effects of very high energy illuminations are detected only under the illuminated surfaces.

The variation of the photo-response of GaSb as function of doping levels and injection levels are in complete agreement with the results obtained by M. W. Shura *et.al* by steady-state photoconductivity measurements [32, 33].

Chapter 5

Conclusion

In this thesis, the variation of photon absorption rate at different positions inside the bulk and thin films of Gallium antimonide (GaSb) semiconductor were determined for illuminations of different energies. Then, the total absorption rate of photons with different energies is described in samples of different thicknesses. While computing, multiple reflections of the photons from the top and the bottom surfaces into the bulk of the material are considered. Next, the photo-response to the illumination by the material that has an inverse relationship with the absorption effect in the material is determined in terms of the radiative excess minority carrier lifetime as function of the depth below the illuminated surface and the thicknesses of the samples for photons with different energies and injection levels in samples with different doping concentrations. In order to clearly understand the effects of the energy and the injection level of the photo-response of the material, the analysis is performed by varying the injection level and the energy of the illumination independently.

The results of the analysis the effects of the absorption of photons in thin films show that, when a point at a depth, x below the illuminated surface is illuminated by photons of different energy, only a photon with absorption coefficient equal to the reciprocal of x has relatively very large absorption rate of as compared to other photons. The absorption rate at the absorption depth of a photon is equal to 37% of its maximum absorption rate under the illuminated surface. High energy photons are found to be absorbed more near the illuminated surface and photons with very low energies are passing through the materials without being absorbed (or with a few absorption effect). Since, the reduction in the photon absorption rate occurred in the bulk semiconductor is compensated in thin films due to the multiple reflections of photons from the top and the bottom surfaces into the film, each point inside a thin film semiconductor has more photon absorption rate as compared to the corresponding points in thick semiconductors. The total photon absorption rate in the entire material is also increases with decreasing the thickness of the films. Photons with very high energies are absorbed at very high rate in very thin films and photons with very low energy are passing unabsorbed (with less absorption) through the materials. The variation of

absorption rate with the energy of the illumination is very high in thin films than in thick films, whereas, the variation of absorption rate with the samples thickness is very high for high energy photons than for low energy photons.

The results of the analysis of the excess carriers lifetime confirms that, the depletion of thermal equilibrium majority carrier concentration enhances the magnitude of the low injection level excess carrier lifetime in the under surface depletion layer than in the deep bulk. The magnitude of the radiative excess minority carrier lifetime is highly decreasing in the deep bulk of the semiconductor with increasing the doping level, while the magnitude of the radiative excess minority carrier lifetime under the surface is insensitive to the doping level. This is evidence for the premise that, the surface property is unaltered by the doping effect of the material and the surface Fermi level position is pinned regardless of the doping level of the sample. The effects of high injection level and low energy photons can be detected equally at all points inside a thin film material, while the effects of the low injection level and low energy photons cannot be detected in the deep bulk, but can be detected under the top and the bottom surfaces. The effects of an illumination with high energy and high injection level can be detected at different points inside a material with various photo-responses. However, the effect of an illumination with high energy and low injection level can be detected only under the illuminated surface.

References

[1] Bach et al., ""Thin Film on Glass"," in *springer*, Verlag, 2003.

[2] Amanuallah et al., "Co-activation effect of chlorine on the physical properties of CdS thin films prepared by CBD technique for photovoltaic applications," *Applied Research,* 2005.

[3] Khallaf, H.et.al, "Insitu boron doping of chemical-bath deposition Cds thin films," *physical solid state,* pp. 256-262, 2009.

[4] Ammanullah et al., "Co-activation effects of chlorine on the physical properties of CdS thin films prepared by CBD technique for photovoltaic applications," *Applied Research,* 2005.

[5] Shadia et al., "Argon and nitrogen implantation effects on the structural and optical properties of vacuum evaporated cadmium sulphide thin films," in *semiconductor science Technology*, 2008, pp. 97-103.

[6] Goswami, A., "Thin Film Fundamentals," New Age International pvt ltd, 2008.

[7] Abusafe et al., "chlorine doped CdS thin films from CdCl2 mixed CdS powder," *Electronic materials,* pp. 128-134, 2004.

[8] Nasr et al., "Effects of pH on the properties of ZnS thin films grown by chemical bath deposition," *Thin film solids,* pp. 4-8, 2006.

[9] Yamaguchi,T., "preparation and characterization of (Cd,Zn)S thin films by chemical bath deposition for photovoltaic devices," *Thin solid films,* vol. 70, pp. 344-516.

[10] Vigil,Galan,O. , "Physical properties of CdS thin films grown by different techniques," in *A comparative study.proceeding of 29 IEEE photovoltaic's specialist conference, 624-628*, 2002.

[11] Oumous,H. and Hadiri,H., "Optical nd electrical properties of annealed CdS thin films obtained from a chemical solution," *thin film solids,* vol. 386, pp. 87-90, 2001.

[12] Chapin,M.and Pearson,L., "A new silicon p-n junction photo cell for converting solar cell for converting solar radiationin to electrical power," *Journal of Applied physics* , p. 676, 1954.

[13] Schroder, K., Semiconductor material and device characterization, New york: John Wiley and sons, 1998.

[14] Siu,C. and Kwok,L., "CuS/CdS thin film solar cells using chemicaliy sprayed CdS films.," *Journal of physics* , vol. 11, p. 58, 1978.

[15] M.Grundman , "The physics of semiconductors," Berlin, Heidelberg, 2006.

[16] Yacobi, B.G., "semiconductor materials an introduction to Basic principles," springer publications, 2003.

[17] S.K.Ghandhi, "semiconductor power devices," New York, Wiley, 1977, pp. 8-9.

[18] S.N.Singh, R.Gandotra, P.K.Singh and B.C.Chakravarty, "Application of photoconductivity decay and photocurrent generation methodes for determination of minority carrier lifetime in silicon," pp. 3-4, 2012.

[19] W.Orton and P.blood , "The electrical characterization of semiconductors-Measurement of minority carrier properties," *Acadamic press limited,* 1990.

[20] Richard H.Bube , Photo electronic properties of semiconductors, Cambridge University press, 1992.

[21] S.Thirumavalavan et al., "Investigations on the photoconductivity studies of Znse,Zns and Pbs thin films," p. 4, 2015.

[22] Omar,M., Elementary solid state physics, London: Wisley and sons, 1975.

[23] C.Kittel, Introduction to solid state physics, John Wiley and Sons,Inc., 2005.

[24] Varshni,V.P., "Band to band radiative recombination in groups IV,VI,and III-V semiconductors," *physica status solidi,* vol. 19, pp. 459-514, 1967.

[25] Thomas R.Harris, "Optical properties of Si, Ge,GaAs, InAs and InP at elevated tempratures," 2010.

[26] Scott C. Phillips, "Optical characterizaion and modeling of compositionally matched Indium Arsenide-Antimonide bulk and multiple Quantum well semiconductors," 2004.

[27] Abdullah, S., "preparation and characterisation of chlorine doped cadmium sulphide thin films and their applications in solar cells," M.sc thesis, kings university, saudi Arabia, 2007.

[28] Ohring, M., "The materials science of thin films," New york, London Academic press Ltd., 1990.

[29] Silva, F., "Impurity cluster effects in high and low doping semiconducotors," *Wiley international journal of Quantum chemistry,* pp. 1-6, 2010.

[30] Omar, M., Elementary solid state physics, London: Wisley and sons , 1975.

[31] John Frederick Roller, "Contactless spectral-dependent measurement of bulk lifetime and surface recombination velocity in silicon photovoltaic materials," p. 55, 2016.

[32] M.W.Shura et al., "Non-linear injection level dependence of the excess carrier life time of P-type Gasb thin films:A two layer model," *Journal of Applied physics,* pp. 1-2, 2012.

[33] M.W.Shura et al., "Photoconduction spectroscopy of p-type GaSb films," *Physica B,* pp. 1-2, 2011.

[34] Grove,A.S., "physics and Technology of semiconductor Devices," John Wiley and sons, 1967.

[35] A.Chandola,R.Pino and P.S.Dutta, "Below band gap optical absorption in the tellurium-oped GaSb," *semiconductor science and Technology,* p. pp 2, 2005.

[36] "http: //www.electronic materials .Usask.ca," [Online].

[37] Rehr et al., "Intrinsic and extrinsic losses in x-ray absorption fine structure (XAFS)," *de Physique Archives,* pp. 97-98, 1997.

[38] T.S.Moss,G.T.Burrell and B.Ellis, semiconductor opto electronics, New york: John Wiley and sons, 1973.

[39] R.K.Lal, P.Chakrabarti, "A comparison of dominant recombination mechanisms in n-type InAsSbmaterials," 2006.

[40] Wolf gang Jacob et.al, "Infrared analysis of thin film :amorphous,hydrogenated carbon on silicon," pp. 2-4, 2000.

[41] Ben G. Streetman and Sanjay Kumar Banerjee, Solid -state Electronic Devices, New Delhi: Asoke K. Ghosh, 1995.

[42] Shockley,W. and Read,W.T., "statistical of the recombination of holes and electrons," *physical review 87(5),* pp. 835-842, 1952.

[43] V.K.Khanna, "carrier life times and recombination -generation mechanisms in semiconductor device physics," *solid state devices division,* pp. 223-224, 2004.

[44] T.Trupke, M.A.Green, P.Wurfel, P.P.Altermatt, A.Wang, J.Zhao, and R.Corkish, "Temperature dependence of theradiative recombination coefficient of intrinsic crystalline silicon," *J.Appl.Phys.,* vol. 94, pp. 4930-4937, 2003.

[45] M.J.Kerrar, "Surface, Emitter and Bulk recombination in silicon and Development of silicon nitride passivated solar cells," pp. 6-8, 2002.

[46] Daniel Macdonald, "measuring and interpreting the life time of silicon wafers," *sonar energy,* pp. 255-262, 2004.

[47] A.Rogalski, K.Adamiec,J.Rutkowski, "Narrow -gap semiconductor photodiodes," USA, SPIE press, 2000.

[48] Dieter K. Schroder, "Carriers lifetime in silicon," *IEEE Transactions on electron devices,* vol. 44, 1997.

[49] R.Sinton and T.Mankad , "contactless carrier lifetime measurement in silicon wafers," *Ingots nd Blocks,* pp. 1-14, 2010.

[50] P.W.Chye, I.A.Babalola, T.Sukegawa and W.E.Spicer, "GaSb surfaces states and Schotty-Barrier pinning," 1975.

[51] R.N.Hall , "Recombination processes in semiconductors," 1959.